AGU PUBLICATIONS

JGR

Journal of Geophysical Research: Biogeosciences

RESEARCH ARTICLE

10.1002/2017JG004361

Climate Change Impacts on Net Ecosystem Productivity in a Subtropical Shrubland of Northwestern México

Vivian S. Verduzco[1,2], Enrique R. Vivoni[2,3], Enrico A. Yépez[1], Julio C. Rodríguez[4], Christopher J. Watts[5], Tonantzin Tarin[1,6], Jaime Garatuza-Payán[1], Agustin Robles-Morua[1], and Valeriy Y. Ivanov[7]

[1]Departamento de Ciencias del Agua y Medio Ambiente, Instituto Tecnológico de Sonora, Ciudad Obregón, México, [2]School of Earth and Space Exploration, Arizona State University, Tempe, AZ, USA, [3]School of Sustainable Engineering and the Built Environment, Arizona State University, Tempe, AZ, USA, [4]Departamento de Agricultura y Ganadería, Universidad de Sonora, Hermosillo, México, [5]Departamento de Física, Universidad de Sonora, Hermosillo, México, [6]School of Life Sciences, University of Technology Sydney, Sydney, New South Wales, Australia, [7]Department of Civil and Environmental Engineering, University of Michigan, Ann Arbor, MI, USA

Key Points:
- Model simulation accurately captured the seasonality of vegetation activity
- Net ecosystem productivity decreased under reduced summer rainfall and increased temperature scenarios
- Elevated CO_2 scenarios offset the negative impacts of meteorological conditions

Correspondence to:
E. R. Vivoni,
vivoni@asu.edu

Citation:
Verduzco, V. S., Vivoni, E. R., Yépez, E. A., Rodríguez, J. C., Watts, C. J., Tarin, T., et al. (2018). Climate change impacts on net ecosystem productivity in a subtropical shrubland of northwestern México. *Journal of Geophysical Research: Biogeosciences*, *123*, 688–711. https://doi.org/10.1002/2017JG004361

Received 14 DEC 2017
Accepted 9 FEB 2018
Accepted article online 20 FEB 2018
Published online 28 FEB 2018

Abstract The sensitivity of semiarid ecosystems to climate change is not well understood due to competing effects of soil and plant-mediated carbon fluxes. Limited observations of net ecosystem productivity (NEP) under rising air temperature and CO_2 and altered precipitation regimes also hinder climate change assessments. A promising avenue for addressing this challenge is through the application of numerical models. In this work, we combine a mechanistic ecohydrological model and a soil carbon model to simulate soil and plant processes in a subtropical shrubland of northwest México. Due to the influence of the North American monsoon, the site exhibits net carbon losses early in the summer and net carbon gains during the photosynthetically active season. After building confidence in the simulations through comparisons with eddy covariance flux data, we conduct a series of climate change experiments for near-future (2030–2045) scenarios that test the impact of meteorological changes and CO_2 fertilization relative to historical conditions (1990–2005). Results indicate that reductions in NEP arising from warmer conditions are effectively offset by gains in NEP due to the impact of higher CO_2 on water use efficiency. For cases with higher summer rainfall and CO_2 fertilization, climate change impacts lead to an increase of ~25% in NEP relative to historical conditions (mean of 66 g C m^{-2}). Net primary production and soil respiration derived from decomposition are shown to be important processes that interact to control NEP and, given the role of semiarid ecosystems in the global carbon budget, deserve attention in future simulation efforts of ecosystem fluxes.

1. Introduction

Although the carbon sink strength of semiarid ecosystems is still under debate (Xiao et al., 2011), recent studies have recognized that these areas have a dominant role, stronger than other biogeographic regions, in regulating the intra-annual and interannual variability of the global carbon cycle (Ahlström et al., 2015; Poulter et al., 2014). A transition to more arid conditions (e.g., increasing temperatures and prolonged drought spells) in these regions (Pachauri et al., 2014; Seager et al., 2007) will have implications on the productivity of semiarid ecosystems. This is the case for most of the North American monsoon (NAM) region, which comprises semiarid areas in the southwestern United States and northwestern México (Douglas et al., 1993; Vivoni et al., 2008). The NAM system is a pronounced increase in precipitation during the warm season (July–September) leading to increased biological activity (Flato et al., 2013; Forzieri et al., 2014). Remote sensing analyses have quantified the spatial and temporal variability of vegetation greening during the NAM (e.g., Tang et al., 2012; Watts et al., 2007). However, ecosystem processes regulating the carbon cycling are not understood well enough to anticipate the implications of climate change on the net carbon balance of these semiarid ecosystems.

The eddy covariance (EC) technique has become a useful approach for measuring water, energy, and carbon fluxes at the ecosystem level (Baldocchi et al., 2001), with several studies conducted in different ecosystems in the NAM region (e.g., Anderson & Vivoni, 2016; Méndez-Barroso et al., 2014; Pérez-Ruiz et al., 2010; Scott et al., 2010, 2015; Yépez et al., 2007). By quantifying carbon dioxide (CO_2) exchanges between ecosystems and the overlying atmosphere (Loescher et al., 2003), net ecosystem productivity (NEP) can be measured via the EC method as a degree of the metabolic activity of a terrestrial ecosystem. Furthermore, traditional flux partitioning models have been applied to estimate NEP components, gross primary productivity (GPP)

and ecosystem respiration (R_{ECO}) (Reichstein et al., 2005, Stoy et al., 2006). Since NEP consists of the difference between GPP and R_{ECO}, its response to hydrometeorological conditions has been difficult to identify (Biederman et al., 2016; Nayak et al., 2015; Scott et al., 2015). This is primarily due to the differential sensitivity of GPP and R_{ECO} to changes in temperature and precipitation (e.g., Euskirchen et al., 2014; Shi et al., 2014). As a result, semiarid ecosystem responses to climate change remain highly uncertain. On the one hand, GPP may be reduced by warming via plant heat stress (Sage & Kubien, 2007) and via stomatal closure from increased evaporative demand and reductions of soil water content (SWC) (Seneviratne et al., 2010; Williams et al., 2013) affecting vegetation productivity (Novick et al., 2016). For instance, Biederman et al. (2017) found that warm temperatures have a negative effect on NEP in semiarid ecosystems of southwestern North America. Stomata respond to transpiration rates in a process known as the apparent "feed forward response", implying that transpiration strongly decreases at high vapor pressure deficit, particularly during periods of water stress (Duursma et al., 2014; Novick et al., 2016). When stomata close in this manner, carbon assimilation and GPP decrease, thus reducing NEP. Photosynthetic enhancements due to rising CO_2 atmospheric concentrations (Smith et al., 2000) and the lengthening of the growing season (Kunkel, 2016), however, may increase GPP. These changes are known to affect ecosystem water use efficiency (WUE = GPP/evapotranspiration (ET)), a measure of the sensitivity of photosynthesis rates to changes in hydroclimatic conditions (Yang et al., 2016). In addition, changes in rainfall timing, intensity, and distribution are also important factors affecting NEP, though the net effect or directionality are unclear (Allard et al., 2008; Gherardi & Sala, 2015; Heisler-White et al., 2008; Miranda et al., 2011; Robertson et al., 2009; Rohr et al., 2013; Ross et al., 2012; Xie et al., 2015).

Similarly, the effects of climate change on R_{ECO} in semiarid ecosystems are uncertain due to complex dynamics occurring during periods of water availability (Collins et al., 2014; Fan et al., 2012). R_{ECO} integrates plant (autotrophic) and microbial (heterotrophic) processes that are coupled (Sacks et al., 2007; Verduzco et al., 2015) and has been shown to increase, decrease, or remain unchanged under warming conditions (Arnone et al., 2008; Lenton & Huntingford, 2003; Luo et al., 2001; Zhou et al., 2007). R_{ECO} is also highly variable under different precipitation conditions (Cable et al., 2008; Harper et al., 2005; Thomey et al., 2011). Some studies have found that warming can substantially increase cellular metabolic maintenance (e.g., Amthor, 1984; Ryan, 1991), which in turn affects autotrophic respiration (R_a). Although studies have shown that plants can acclimate to increasing temperatures (Slot & Kitajima, 2015), the degree of and time to acclimation for different plant functional types is still unknown (Drake et al., 2015; Yamori et al., 2014). Furthermore, heterotrophic respiration has been observed to respond positively to temperature (Lloyd & Taylor, 1994), but its sensitivity has been related to limiting factors such as substrate availability and quality, which are coupled to primary productivity (Sponseller, 2007; Zhou et al., 2013) and SWC (Conant et al., 2004; Davidson et al., 2006; Liu et al., 2009).

Given the uncertainties in quantifying the net carbon response of semiarid ecosystems to climate change, a useful approach for addressing this problem is by combining ecosystem level measurements and numerical modeling. Previous efforts have found misrepresentation in the modeling of semiarid ecosystem carbon fluxes (e.g., Huntzinger et al., 2012; Vargas et al., 2013), net carbon balance (Keenan et al., 2012), and its responses to climate change (Friedlingstein et al., 2014). While simulating water, energy, and carbon fluxes remains challenging in semiarid ecosystems (Fisher et al., 2014; Li et al., 2004; Xu et al., 2013), there has been much progress on coupled water-vegetation model representations in recent years (Fatichi, Pappas, et al., 2016). Included in these advances are more accurate representations of ecosystem processes at shorter temporal scales and the simulation of longer-term phenological variations for different plant functional types (e.g., Ivanov et al., 2008a, 2008b). In addition, finer representations of event-scale and seasonal precipitation effects on vegetation dynamics have been achieved, leading to plant carbon assimilation into a number of pools that are essential for capturing vegetation dynamics (e.g., Fatichi, Pappas, et al., 2016; Ivanov et al., 2008a, 2008b). Given the importance of heterotrophic respiration in semiarid ecosystems (Cable et al., 2008; Verduzco et al., 2015; Yépez et al., 2007), an appropriate representation of this process is necessary for simulating the annual cycle and interannual variability of NEP as well as identifying the impacts of different climate change drivers (e.g., rising CO_2 and changing meteorological conditions).

In this contribution, we combine the mechanistic ecohydrological model of Ivanov et al. (2008a) (TIN-based Real-time Integrated Basin Simulator—Vegetation Generator for Interactive Evolution, tRIBS-VEGGIE, model)

with the soil carbon model (SCM) of Porporato et al. (2003) to describe ecosystem plant and soil processes (e.g., GPP and autotrophic and heterotrophic respiration) controlling NEP in a subtropical shrubland in northwestern México. In contrast to prior efforts (e.g., terrestrial biosphere models, Huntzinger et al., 2012), the combined tRIBS-VEGGIE and SCM approach tracks energy, water, temperature, and substrate limitations on photosynthesis and respiration from multiple carbon pools using process-level prognostic equations that are tailored to seasonally dry ecosystems. We use a 5 year long record of EC flux and meteorological data (Méndez-Barroso et al., 2014; Villarreal et al., 2016) from a subtropical shrubland as well as remote sensing products to calibrate and test the model simulations for its ability to realistically capture water fluxes, vegetation dynamics, and the components of net ecosystem productivity (NEP = GPP $- R_{ECO}$). After model confirmation, we conduct a series of climate change experiments using long-term forcing generated by the stochastic downscaling of a set of climate projections from Taylor et al. (2012) that represent near-future (2030–2045) meteorological and atmospheric CO_2 conditions as well as a historical forcing data set of equivalent length (1990–2005). We selected the near-future period to avoid the potential for dramatic changes in ecosystem composition due to climate change impacts. Combining tRIBS-VEGGIE and SCM within the climate change experiments allowed us to pose the following questions: (1) What are the mechanisms through which soil-plant processses control NEP in seasonally dry, semiarid ecosystems? (2) What, if any, will be the impacts of climate change on NEP and its components in the subtropical shrubland? and (3) What is the net effect of projected changes in meteorological conditions and atmospheric CO_2 on NEP? As a result, this study aims to understand the potential effects of climate change on ecosystem dynamics and carbon cycling in semiarid areas experiencing strong seasonality.

2. Materials and Methods

2.1. Site Description

The study site is a subtropical shrubland located ~120 km northeast of Hermosillo, Sonora, México (29.74°N, 110.53°W) near the rural town of Rayón at an elevation of 632 m. The local climate is semiarid (Köppen classification BSh) with hot summers and cool winters. The long-term (1961–2009) average annual temperature and precipitation (±1 standard deviation) are 21.4 ± 6.4°C and 487 ± 181 mm yr^{-1}, as obtained from Comisión Nacional del Agua station 00026181 at Rayón, Sonora. Conditions during the study period (2008–2012) were similar to the long-term average, with a mean annual air temperature (TA) of 22.7 ± 0.6°C and precipitation (P) of 481 ± 92.8 mm yr^{-1}. Precipitation during the NAM season (July–September) is approximately 76% of the annual total at the site (Vivoni, Rodríguez, et al., 2010) leading to a peak in vegetation greenness in the month of August (Méndez-Barroso et al., 2009). Site vegetation is composed of drought-deciduous trees and shrubs, including torote papelío (*Jatropha cordata*), tree ocotillo (*Fouquieria macdougalii*), acacia (*Acacia cochliacantha*), palo verde (*Parkinsonia praecox*), Mexican mimosa (*Mimosa distachya*), and velvet mesquite (*Prosopis velutina*) as well as organpipe cactus (*Stenocereus thurberi*). Brown (1994) described the vegetation characteristics of subtropical shrublands (or Sinaloan thornscrub) in greater detail. The site topography is relatively flat in proximity to the EC tower (Vivoni, Watts, et al., 2010), while the soils are shallow (~1 m) and classified as regosol-yermosol (INEGI, 2010) with sandy loam (0 to 30 cm) and sandy clay (30 to 100 cm) texture. Prior studies further describe the site properties used here for the model application, including the soil hydraulic properties, the vegetation albedo, and structural properties (e.g., Méndez-Barroso et al., 2014; Vivoni, Rodríguez, et al, 2010; Vivoni, Watts, et al., 2010).

2.2. Site Measurements

Meteorological flux measurements were performed using the EC technique (Baldocchi, 2003, 2008) using a three-dimensional sonic anemometer (CSAT-3, Campbell Sci.) and an open-path infrared gas analyzer (LI-7500, Li-COR Inc.) placed on a 9 m tower over the tree canopy of around 6 m height and oriented with the prevailing southwest wind direction. Vivoni, Watts, et al. (2010) describes the EC installation at the site, including the characteristics of the footprint area. Water vapor and CO_2 concentrations and TA were measured at high frequency (20 Hz), collected with a CR5000 datalogger (Campbell Sci.) and processed to 30 min averaged quantities to obtain latent (LE) and sensible heat flux (H) and net ecosystem exchange (NEE) of CO_2, as described in the following section. By convention, negative NEE values indicate ecosystem

carbon uptake from the atmosphere, which correspond to a positive net ecosystem productivity (i.e., −NEE = NEP). Net radiation (R_{net}) was measured using a CNR Lite2 (Kipp and Zonen) radiometer, and incoming solar radiation with a CMP3 radiometer (Campbell Sci.).

For use in the model, incoming solar radiation was partitioned into direct and diffuse components of the visible (VIS, 0.4–0.7 μm) and near-infrared (NIR, 0.7–1.3 μm) bands following the procedures of Spitters et al. (1986), while incoming longwave radiation was estimated as a function of TA (Duarte et al., 2006). A humidity and TA sensor (HMP45D, Vaisala) was used to obtain vapor pressure (VP) and TA. Volumetric SWC was obtained as the average of two reflectometer (CS616-L, Campbell Sci.) measurements at a 10 cm depth over the period 2008–2010 and from a soil moisture sensor (ECH2O probe, Decagon Devices) at the same depth and location for portions of 2012. No additional soil moisture sensors at larger soil depths were available. Local precipitation was measured with a tipping-bucket rain gauge (TB4, Hydrological Services). All meteorological measurements were recorded as 30 min averages within the CR5000 datalogger and averaged to hourly inputs for the model applications. Additional information on measurements is presented by Méndez-Barroso et al. (2014), Villarreal et al. (2016), and Vivoni, Rodríguez, et al. (2010).

Several data gaps occurred during the 2008–2012 period (i.e., 15 to 26% of measurements during all years, except 2008 with 63% missing data since observations started in the summer). We followed the procedure of Robles-Morua et al. (2012) to fill in the necessary meteorological forcing. This process consisted of bias-correcting the surface meteorological data obtained from the North American Land Data Assimilation System (NLDAS) (Mitchell et al., 2004) in the grid pixel (12 km) corresponding to the study site during periods of simultaneous ground data. Linear corrections were applied to hourly variables of atmospheric pressure, incoming solar radiation, and vapor pressure, while TA was corrected using the adiabatic lapse rate (6.5°C km^{-1}) to match the site elevation. A logarithmic profile adjustment was used to modify the 10 m NLDAS wind speed to 2 m height assumed for all forcing variables in the ecohydrological model (tRIBS-VEGGIE). The use of bias-corrected NLDAS products to gap-fill the ground-based data was deemed important to create a continuous series of meteorological forcing.

In addition, we utilized remotely sensed data from the Moderate Resolution Imaging Spectroradiometer (MODIS; ORNL DAAC, 2008) to test the model representation of vegetation dynamics, following Méndez-Barroso et al. (2014). Cloud-free composites of the Normalized Difference Vegetation Index (NDVI, 16 day, 250 m, MOD13Q1) and leaf area index (LAI, 8 day, 1 km, MOD15A2) were linearly interpolated to a daily product for this purpose. Due to its higher temporal resolution, we report the model evaluation against LAI for assessing vegetation dynamics. Previous research in semiarid areas has found good agreement between ground-based vegetation conditions and MODIS (i.e., Fensholt et al., 2004; Jenerette et al., 2010), but it should be noted that there are discrepancies between the site conditions and inferred variables of the remote sensing products due to different spatiotemporal resolutions and sometimes due to scattering and absorption by the atmospheric composition (Nagol et al., 2009).

2.3. Flux Quality Control and Partitioning

Conventional corrections were applied to EC measurements following Scott et al. (2004), including removal of outliers (gas concentrations greater than ±4 standard deviations, Massman, 2001), a correction for density fluctuations (Webb et al., 1980), and the application of the double-rotation method (Wilczak et al., 2001). In addition, friction velocity (u^*) was calculated according to quantitative methods (Scott et al., 2004), and periods of time with a friction velocity less than $u^* = 0.20$ m s^{-1} were filtered (Aubinet et al., 2000; Xu & Baldocchi, 2004) to reduce nighttime flux underestimation (Barr et al., 2013). The u^* threshold was selected such that there is no dependence between nighttime fluxes and friction velocity. Resulting data gaps were filled in following the procedures of the Eddy Covariance Gap-Filling and Flux-Partitioning Tool available at: http://www.bgc-jena.mpg.de/~MDIwork/eddyproc/index.php, following Reichstein et al. (2005). The surface energy balance was evaluated at the study site by Villarreal et al. (2016) over 2008–2010 (a closure of 0.89) and Méndez-Barroso et al. (2014) over summers in 2006–2009 (a closure of 0.75). The partitioning of NEE into its components GPP and R_{ECO} (i.e., NEE = R_{ECO} − GPP) was carried out using the sensitivity of R_{ECO} to TA (Flanagan, Wever, & Carlson, 2002; Reichstein et al., 2005). This NEE partitioning approach has been shown to be consistent with other methods (Babst et al., 2014; Desai et al., 2008).

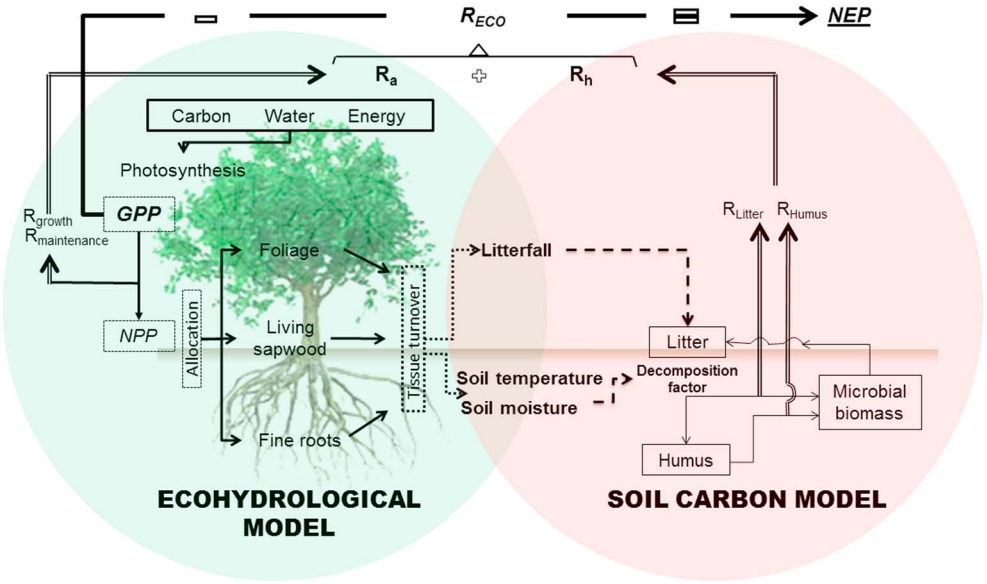

Figure 1. Conceptual diagram of model-based estimation of ecosystem carbon fluxes using tRIBS-VEGGIE and soil carbon model. Dotted lines depict ecohydrological model outputs into the soil carbon model, while double lines specify sources of autotrophic, heterotrophic, and ecosystem respiration ($R_{ECO} = R_a + R_h$). Net ecosystem productivity (NEP) is obtained as GPP $-$ R_{ECO}.

2.4. Ecohydrological and Soil Carbon Modeling

Water, energy, and carbon dynamics at the subtropical shrubland were simulated using a combination of an ecohydrological model (tRIBS-VEGGIE, Ivanov et al., 2008a, 2008b) and a SCM (Porporato et al., 2003) coupled through the production of litter and the soil moisture and temperature conditions (Figure 1). Following prior efforts in semiarid regions (Bisht, 2010; Sivandran & Bras, 2012), a drought-deciduous C3 shrub was used as the plant functional type in the one-dimensional simulations using an irregular subsurface mesh (25 layers over 1 m depth). In addition to vertically resolved soil hydrologic and thermal dynamics, tRIBS-VEGGIE captures a set of biophysical and biochemical plant processes, such as photosynthesis; autotrophic respiration (R_a); carbon allocation to foliage, sapwood, and fine roots; tissue turnover; and vegetation phenology. This allows the estimation of gross and net (NPP = GPP $-$ R_a) primary productivity for the plant functional type. The time-evolving plant conditions are directly affected by and provide an influence on the local energy and water budget in an interactive fashion (Ivanov et al., 2008a, 2008b). Simulated SWC, surface energy fluxes (R_{net}, H, and LE), total ET, and LAI, among others, depend on local meteorological conditions, soil properties, and plant functional traits obtained via local measurements or parameterized through a model calibration and validation procedure. Overall, tRIBS-VEGGIE simulates the dynamic feedbacks between vegetation and its surrounding environment at differing time scales, explicitly represented starting at the scale of a few minutes (e.g., resolving canopy leaf temperatures), to hourly resolution (e.g., stomatal dynamics), and up to the daily scale processes (e.g., plant phenology and leaf turnover). Ivanov et al. (2008a, 2008b) provide additional details on the model biophysics and its application in other semiarid settings.

As depicted in Figure 1, tRIBS-VEGGIE does not simulate soil heterotrophic respiration (R_h), limiting its ability to represent net ecosystem productivity (NEP = GPP $-$ R_a $-$ R_h). To address this, we implemented a simplified version of the SCM of Porporato et al. (2003) based on three separate carbon pools (litter, humus, and microbial biomass) to track soil organic matter decomposition and heterotrophic respiration (Bolker et al., 1998; Manzoni et al., 2004; Parolari & Porporato, 2016). While this approach does not track nitrogen dynamics, we accounted for C:N effects on decomposition rates through the use of a heuristic factor φ described in Rodríguez-Iturbe and Porporato (2004) and based values either on local data or magnitudes reported for the region (Martínez-Yrízar et al., 2007; Núñez et al., 2001). Daily carbon pool dynamics simulated in the SCM were driven by SWC and temperature conditions and the leaf litter production derived from tRIBS-VEGGIE. As a result, the coupling of tRIBS-VEGGIE and SCM allows for the

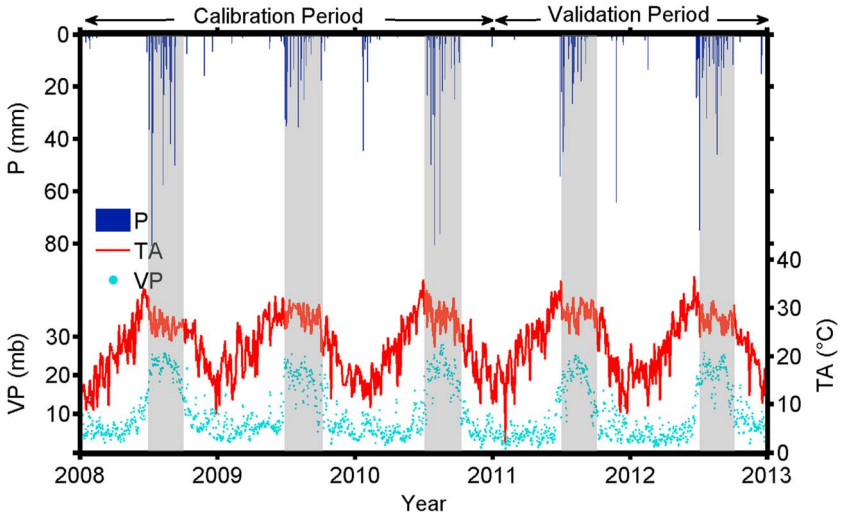

Figure 2. Mean daily meteorological conditions during the study period (2008–2012) consisting of precipitation (*P*), air temperature (TA), and vapor pressure (VP). Shaded areas represent North American monsoon period (July–September) of each year.

effects of vegetation phenology (i.e., leaf senescence and fall) to impact R_h and NEP when soil moisture and temperature conditions are favorable.

2.5. Model Forcing, Parameterization, and Validation

Gap-filled meteorological observations over the period 2008–2012 were aggregated to hourly resolution as forcing for tRIBS-VEGGIE and consisted of atmospheric pressure, vapor pressure, TA, wind speed, incoming solar and longwave radiation, and precipitation. In addition, direct and diffuse radiation components in the visible and near-infrared bands and the average atmospheric CO_2 concentration during 2008–2012 (390 ppm) were input. Figure 2 presents an example of the meteorological forcing, illustrating the strong seasonality in precipitation and its corresponding effects on TA and vapor pressure during the NAM.

The study period was divided into two subsets for model calibration (2008–2010, 1,096 days) and validation (2011–2012, 731 days) based upon matching the subset length when excluding gap-filled periods. While conditions varied to some extent among the subsets, no trends were noted that would impact model calibration and validation. A similar setup was carried out for the SCM by using leaf litterfall, soil moisture, and soil temperature conditions obtained from tRIBS-VEGGIE as inputs (Figure 1). Following Vivoni et al. (2005), the sequence of tRIBS-VEGGIE and SCM simulations were conducted in a periodic fashion by repeating the same 5 year meteorological forcing six times (i.e., total simulation length of 30 years) and retaining the two subsets in the last 5 year period for model calibration and validation purposes. This initialization approach stabilized SWC, soil temperature, and carbon storage amounts in the vegetation (foliage, sapwood, and fine roots) and soil (litter, microbial biomass, and humus) pools, thus reducing transient errors in the assignment of the initial conditions.

Initial model parameterization was conducted for tRIBS-VEGGIE and SCM based upon prior efforts with each model (e.g., Bisht, 2010; Ivanov et al., 2008a; Parolari & Porporato, 2016; Porporato et al., 2003; Sivandran & Bras, 2012), including applications for the subtropical shrubland (Méndez-Barroso et al., 2014; Vivoni, Rodríguez, et al., 2010). For instance, Table 1 presents the soil hydraulic and thermal properties used in tRIBS-VEGGIE for the sandy loam soils at the site whose initial values were obtained through manual calibration conducted by Méndez-Barroso et al. (2014). As in that work, we simplified the modeling of site conditions by treating the soil profile as a uniform sandy loam. In contrast to Méndez-Barroso et al. (2014), however, we applied the one-dimensional Richards equation using a finite element, backward Euler time stepping numerical approximation for infiltration into the unsaturated soil profile (irregular mesh with 25 layers over 1 m depth), as detailed in Ivanov et al. (2008a). Accordingly, modifications to the soil parameters within feasible ranges based on pedotransfer functions from Rawls et al. (1982) were required to match a larger set of

Table 1
Soil Parameters

Soil type	Sandy loam
K_s	55
θ_s	0.45
θ_r	0.02
λ_o	0.47
ψ_b	−90
$k_{s,dry}$	0.214
$k_{s,sat}$	2.64
C_s	1,610,586

Note. K_s (mm h^{-1}) = surface hydraulic conductivity; θ_s (–) = saturated moisture content; θ_r (–) = residual moisture content; λ_o (–) = pore size distribution index; ψ_b (mm) = air entry bubbling pressure; $k_{s,dry}$ and $k_{s,sat}$ (J m^{-1} s^{-1} K^{-1}) = heat conductivity for dry and saturated soils; C_s (J m^{-3} K^{-1}) = heat capacity of dry soils.

observations (SWC, R_{net}, H, LE, and LAI) over a longer period (i.e., three continuous years in the calibration period).

An invariant rooting profile extending to 1 m depth and a vegetation fraction (v_f = 0.6) were estimated for the study site following Jackson et al. (1996) and Méndez-Barroso et al. (2014). In addition, tRIBS-VEGGIE required a larger set of model parameters to describe biochemical, biophysical, interception, phenological, carbon allocation, and water uptake processes (Ivanov et al., 2008a). Table 2 lists the final parameter values for vegetation processes and indicates their sources as from literature (L), observation (O), or calibration (C).

Manual calibration of vegetation parameters focused on capturing the LAI dynamics during 2008–2010 as observed from MODIS during the NAM growing season. A one-at-a-time sensitivity analysis was conducted to identify the importance of each parameter on the simulation of LAI and limit the sampling necessary for model calibration. Similarly, a manual calibration approach was used for the SCM parameters (Table 3). We used observations of SCM model parameters or initial conditions when available from the site or nearby areas (e.g., Búrquez et al., 1999; Martínez-Yrízar et al., 1999, 2007; Núñez et al., 2001; Pavón et al., 2005). Though manual calibration was conducted, the combined models are amenable to automated estimation methods (e.g., Duan et al., 1993) due to the low computational demands for single-site applications. The combination of tRIBS-VEGGIE and SCM allowed for simulation of $R_{ECO} = R_a + R_h$ that was compared to R_{ECO} observations derived from the EC method during calibration and subsequently permitted a comparison of NEP between observations and simulations. We validated the model performance using a comparison between simulated and observed values of the aforementioned variables during the 2011–2012 period, which was not used in the model calibration effort.

2.6. Climate Change and CO_2 Fertilization Experiments

We obtained TA (monthly) and precipitation (3 h) projections from the Coupled Model Intercomparison Project version 5 (CMIP5) (Taylor et al., 2012) for three General Circulation Models (GCMs) selected for their ability to represent the NAM system (Geil et al., 2013): CNRM-CM5, HadGEM2-ES, and MIROC5. Single realizations from each model were selected for a near-future period (2030–2045) under the RCP8.5 emissions case (IPCC, 2013), selected to match the 15 year length of a historical forcing period (1990–2005) obtained from NLDAS (labeled as "HIST"). Given the hourly meteorological forcing requirements of tRIBS-VEGGIE, we implemented the stochastic downscaling method of Fatichi et al. (2013) to apply a set of factors of change derived from the individual GCMs and their averaged conditions (referred to hereafter as "AVE") to the statistical properties obtained from the historical forcing. For each scenario, sets of change factors were calculated separately for the statistical properties of precipitation (e.g., mean, variance, skewness, and frequency of no precipitation at different aggregation periods (1, 6, 24, and 72 h) and mean monthly TA). Since GCM realizations were obtained at a 3 h interval, we followed Fatichi et al. (2011) to extend the statistical properties to a finer hourly resolution for the full set of meteorological forcings (atmospheric pressure, wind speed, incoming solar and longwave radiation, TA, vapor pressure, and precipitation). Since our study periods were relatively short (15 years), we utilized the derived statistical metrics from the method of Fatichi et al. (2013) to generate synthetic (100 years long) hourly forcings for each scenario (HIST, CNRM-CM5, HadGEM2-ES, MIROC5, and AVE). These should be considered as representative realizations of the climate system under stationary historical and near-future conditions, as simulated by these GCMs, allowing statistical sampling to be conducted. Two sets of simulations were performed for each scenario to differentiate the effects of CO_2 fertilization from meteorological changes: (1) No fertilization cases used the average of 365 ppm calculated from historical CO_2 concentrations from 1990–2005 and (2) CO_2 fertilization cases with a constant concentration of 482 ppm, obtained from RCP8.5 from 2030–2045 period (about a 32% increase in CO_2 above historical). Since we are simulating synthetic 100 year long scenarios, it was necessary to use a constant CO_2 concentration that best represents the conditions for each period (i.e., 1990–2005 and 2030–2045).

Table 2
Vegetation Parameters

Parameter	Value	Source
Biochemical processes		
V_{max25}	50	C
K	0.2	C
m	9	L
b	10,000	L
$\varepsilon_{3,4}$	0.08	L
r_{sapw}	9.61×10^{-10}	L
r_{root}	1.09×10^{-8}	L
w_{grw}	0.25	L
d_{leaf}	1	L
d_{sapw}	0.04	L
d_{root}	0.33	L
Biophysical and interception processes		
χL	0.01	L
α_{leaf} (VIS, NIR)	0.1, 0.45	L
α_{stem} (VIS, NIR)	0.16, 0.39	L
τ_{leaf} (VIS, NIR)	0.05, 0.25	L
τ_{stem} (VIS, NIR)	0.001, 0.001	L
K_c	0.18	L
g_c	3.9	L
S_{la}	0.011	O
Phenology, allocation, and uptake processes		
γW_{max}	10	C
b_w	2.5	C
γC_{max}	7	C
b_c	1	C
T_{cold}	15	C
e_{leaf}	0.25	L
e_{sapw}	0.1	L
e_{root}	0.65	L
ω	0.8	L
ε_s	2	L
ξ	1.6	L
T_{soil}	20	C
D_{LH}	10	L
$D_{Tmin,Fav}$	6	C
$f_{c,init}$	0.025	L
L_{init}	0.22	L
ψ^*	−0.1	C
ψ_w	−5	C

Note. V_{max25} (μmol CO_2 m^{-2} leaf s^{-1}) is the maximum catalytic capacity of Rubisco at 25°C; K (–) is the time mean Photosyntetically Active Radiation extinction coefficient parameterizing the decay of nitrogen content in the canopy; m (–) is an empirical slope parameter; b (mmol m^{-2} s^{-1}) is the minimum stomatal conductance; $\varepsilon_{3,4}$ (μmol CO_2 μmol^{-1} photons) is the intrinsic quantum efficiency for CO_2 uptake; r_{sapw} and r_{root} (g C g C^{-1} s^{-1}) are the sapwood and fine root respiration coefficients at 10°C; w_{grw} (–) is the fraction of canopy assimilation less maintenance respiration used for tissue growth; d_{leaf}, d_{sapw}, and d_{root} (yr^{-1}) are the turnover rates for leaf, sapwood, and roots; χL (–) is the departure of leaf angles from a random distribution; α_{leaf} and α_{stem} (–) are the leaf and stem reflectances in the visible and near-infrared bands; τ_{leaf} and τ_{stem} (–) are leaf and stem transmittances in the visible and near-infrared bands; K_c (mm h^{-1}) is the canopy drainage coefficient; g_c (mm^{-1}) is the exponential decay parameter of canopy water drainage; S_{la} (m^2 leaf area kg C^{-1}) is the specific leaf area; γW_{max} and γC_{max} (d^{-1}) are maximum drought and cold-induced foliage loss rates; b_W and b_C (–) are the shape parameters reflecting the sensitivity of canopy to drought and cold; T_{cold} (°C) is the temperature threshold below which cold-induced leaf loss begins; e_{leaf}, e_{sapw}, and e_{root} (–) are the base allocation fractions for leaf, sapwood, and roots; ω (–) is the sensitivity parameter of allocation fractions to changes in light and water availability; ε_s and ξ (–) are parameters controlling the relation between carbon content in the aboveground and belowground biomass; T_{soil} (°C) and D_{LH} (h) are the mean daily soil temperature and day length to be exceeded for the growing season start; $D_{Tmin,Fav}$ (day) is the minimum duration for which the conditions of transition from/to the dormant season have to be continuously met; $f_{c,init}$ and L_{init} (–) are the fraction of the structural biomass and leaf area index used to initiate leaf onset; ψ^* and ψ_w (MPa) are the soil matric potentials at which the stomatal closure and plant wilting begins. L = literature; O = observation; C = calibration.

3. Results and Discussion

3.1. Evaluation of Simulated Water, Energy, and Carbon Dynamics

Simulated water, energy, and carbon states and fluxes in the subtropical shrubland were compared to available observations over the calibration, validation, and full study periods using three metrics: correlation

Table 3
Soil Decomposition Parameters

Parameter	Value	Source
C_l	89	L
C_h	895	L
C_b	25	L
C/N_{litter}	23	O
C/N_{humus}	22	L
$C/N_{biomass}$	8	L
r_h	0.003	L/C
r_r	0.65	L
k_b	0.0000988	C
k_h	2.1×10^{-7}	C
k_l	0.00107	C

Note. C_l, C_h, and C_b (g C m^{-2}) are initial carbon concentrations in the litter, humus, and biomass pools; C/N_{litter}, C/N_{humus}, and $C/N_{biomass}$ (–) are carbon-nitrogen ratios of litter, humus, and biomass; r_h and r_f (–) are fractions of organic matter undergoing humification and of decomposed organic carbon that is respired; k_l, k_h, and k_b (h^{-1}) are first-order kinetic constants of litter, humus, and biomass. L = literature; O = observation; C = calibration.

coefficient (CC), bias (*B*), and mean absolute error (MAE) (Vivoni et al., 2006). Table 4 shows the metrics obtained for daily averaged and hourly values, with a CC near 1, a *B* close to unity, and a low MAE indicating a good match between the observed and simulated variables at both time scales and for all variables. For instance, the simulated surface energy fluxes (R_{net}, *H*, and LE) exhibit a good correspondence to observations, with high CC (> 0.77), *B* near unity (within ± 0.16), and an MAE less than 33 W m^{-2} for hourly and daily values. Figure 3 illustrates the model performance with respect to the surface energy fluxes by comparing seasonal cycles of R_{net}, *H*, and LE over the full study period. Note the dramatic change in the partitioning of R_{net} into *H* and LE upon the onset of the NAM in July, with the arrival of summer storms increasing LE (or ET) substantially. Overall, the ecohydrological model adequately captures monthly variations in the surface energy fluxes, though a consistent underestimation of R_{net} of 14.4 W m^{-2} is noted from December through June due to the lack of simulated vegetation (i.e., a decrease in LAI and a corresponding increase in albedo) affecting the absorption of solar radiation, comparable to prior studies (Ivanov et al., 2008a). In addition, tRIBS-VEGGIE simulation tends to slightly overestimate sensible heat flux from May to August by an average of 12.7 ± 3.8 W m^{-2}, despite adequately capturing the latent heat flux, though the difference is within the monthly standard deviation (error bars) obtained across all years. Overall, monthly, daily, and hourly comparisons demonstrate the robust capability of tRIBS-VEGGIE to capture surface energy fluxes, themselves tied to SWC and vegetation conditions.

Figure 4 presents observed and simulated SWC in the top 10 cm, LAI dynamics and litterfall variations during the calibration and validation periods, and simulated soil temperature (T_{soil}) derived from tRIBS-VEGGIE that are critical inputs to the SCM. Note how the summer rainy season during the NAM leads to increases in SWC that were accurately captured by the model, as described in Table 4, with the tRIBS-VEGGIE model serving as an effective tool to interpolate within periods of observed data gaps. Simulated LAI captured well the primary summer growing season (CC ≥ 0.88, B within 0.06 of unity, MAE ≤ 0.39) and the differences between years.

Table 4
Model Performance Metrics for Daily and Hourly Values

		Calibration period 2008–2010			Validation period 2011–2012			Full period 2008–2012		
	Variable	CC	*B*	MAE	CC	*B*	MAE	CC	*B*	MAE
Daily values	SWC (m^3 m^{-3})	0.86	0.91	0.03	0.93	0.65	0.01	0.86	0.83	0.02
	ET (mm)	0.91	0.81	0.01	0.94	0.89	0.02	0.92	0.84	0.01
	LAI (–)	0.88	1.06	0.39	0.91	1.00	0.36	0.89	1.04	0.38
	R_{net} (W m^{-2})	0.85	0.91	19.46	0.97	0.87	15.05	0.91	0.90	17.70
	LE (W m^{-2})	0.91	0.81	9.22	0.94	0.89	11.2	0.92	0.84	10.01
	H (W m^{-2})	0.76	1.16	16.88	0.82	0.91	18.16	0.77	1.04	17.39
	GPP (g C m^{-2})	0.85	0.92	0.04	0.83	1.16	0.04	0.85	1.05	0.04
	R_{ECO} (g C m^{-2})	0.90	1.09	0.02	0.88	1.16	0.02	0.90	1.12	0.02
	NEP (g C m^{-2})	0.58	0.99	0.03	0.67	0.95	0.03	0.60	0.78	0.03
Hourly values	SWC (m^3 m^{-3})	0.80	0.91	0.03	0.90	0.65	0.01	0.81	0.83	0.02
	ET (mm)	0.86	0.81	0.02	0.79	0.88	0.03	0.83	0.84	0.03
	R_{net} (W m^{-2})	0.96	0.91	28.23	0.97	0.87	31.33	0.96	0.90	29.47
	LE (W m^{-2})	0.86	0.81	15.98	0.79	0.88	22.2	0.83	0.84	18.48
	H (W m^{-2})	0.90	1.16	24.65	0.91	0.91	45.33	0.90	1.04	32.92
	GPP (g C m^{-2})	0.70	1.08	0.07	0.75	1.29	0.05	0.72	1.15	0.06
	R_{ECO} (g C m^{-2})	0.73	1.09	0.04	0.69	1.16	0.04	0.71	1.12	0.04
	NEP (g C m^{-2})	0.58	0.97	0.07	0.63	0.94	0.06	0.60	0.78	0.06

Note. Correlation coefficient (CC), bias (*B*), and mean absolute error (MAE) are calculated for soil water content (SWC), evapotranspiration (ET), leaf area index (LAI), net radiation (R_{net}), sensible heat flux (*H*), gross primary productivity (GPP), ecosystem respiration (R_{ECO}), and net ecosystem productivity (NEP) during calibration, validation, and full periods.

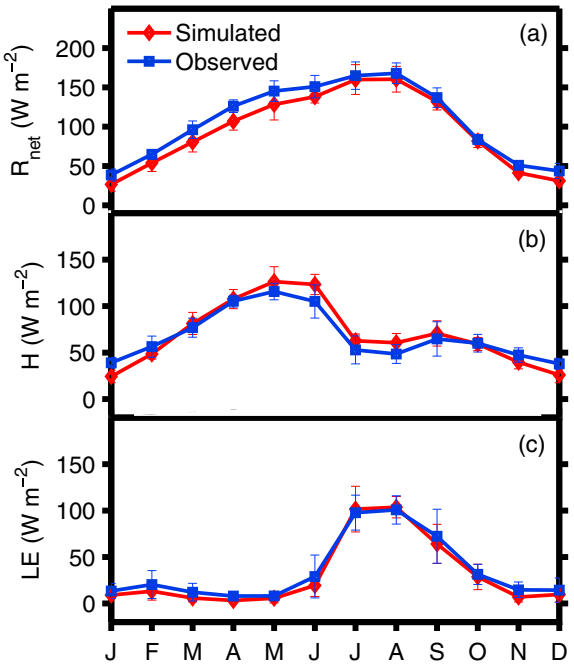

Figure 3. Seasonal cycle of observed versus simulated surface energy fluxes over the study period (2008–2012): (a) net radiation (R_{net}), (b) sensible heat flux (H), and (c) latent heat flux (LE). Symbols are monthly averages and ±1 standard deviation as error bars.

However, the model did not capture the observed (MODIS-based) LAI variations during the winter period, as noted by Bisht (2010). This is likely due to representing only the drought-deciduous component of the ecosystem (C3 shrubland) and possible issues related to the scale discrepancy between MODIS-based LAI estimates and the model application. Although this might lead to small errors in the estimation of annual biomass, the particularly strong summer season minimizes the role played by the winter in terms of physiological activity, as has been noted with carbon fluxes in the NAM region (e.g., Huxman et al., 2004; Pérez-Ruiz et al., 2010; Scott et al., 2004; Verduzco et al., 2015). Correspondingly, model estimates of GPP were adequate at the hourly resolution as compared to derived values from the EC measurements and improved substantially at the daily resolution (Table 4), though we noted that overestimation during the NAM was typical (B = 1.23). Although LAI and the foliage carbon pool appears to have low interannual variations, the simulations of GPP that account for all carbon pools (root, stem, and foliage) correspond well with observations and demonstrate higher values during wetter years, as expected. The few available data on T_{soil} limited the possible tests of the model, though for 2011, tRIBS-VEGGIE matched the observations very well (CC = 0.97, B = 0.99, and MAE = 1.9°C for hourly values).

After the NAM ends, soil moisture and temperature conditions become less favorable for the drought-deciduous plants and the subtropical shrubland transitioned into dormancy (low LAI by November) after a complete foliage turnover (Figure 4). Litterfall was simulated by tRIBS-VEGGIE to account for about 30% of the GPP each year, with values ranging from 120 to 180 g C m^{-2} yr^{-1}, consistent with studies in the Sonoran Desert (~157 g C m^{-2} yr^{-1}) (Martínez-Yrízar et al., 1999). Along with the simulated SWC and T_{soil} conditions, litterfall determined inputs to the SCM from which heterotrophic respiration (R_h) fluxes were simulated (Figure 4b). Simulated carbon amounts in the litter and microbial biomass pools ranged from 20 to 200 g C m^{-2} and from 70 to 130 g C m^{-2}, respectively, whereas the carbon amount in the humus pool remained relatively stable at 895–900 g C m^{-2} during

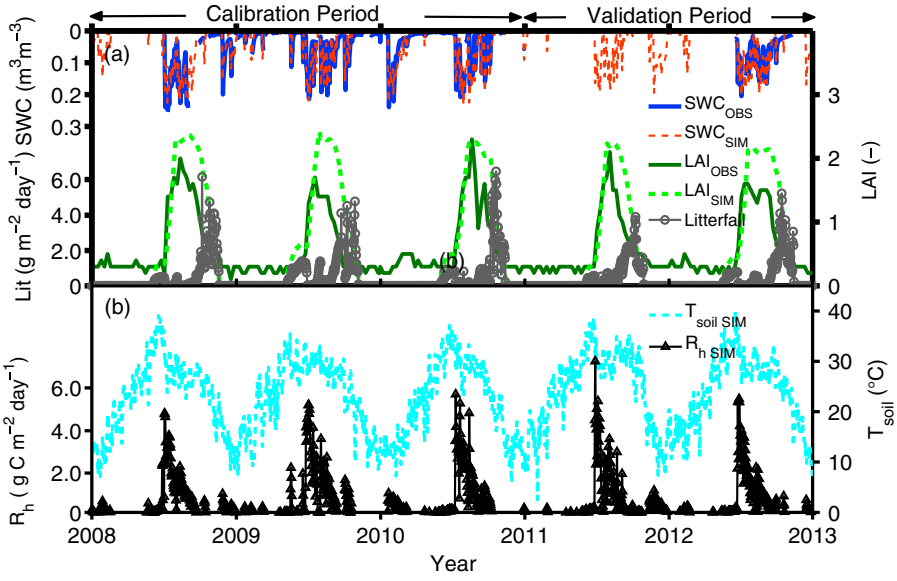

Figure 4. (a) Comparison of daily observed (OBS) and simulated (SIM) soil water content (SWC) and leaf area index (LAI). Simulated litterfall (Lit) in (a), soil temperature (T_{soil}) and heterotrophic respiration (R_h) in (b) from tRIBS-VEGGIE (Litterfall, T_{soil}) and soil carbon model (R_h).

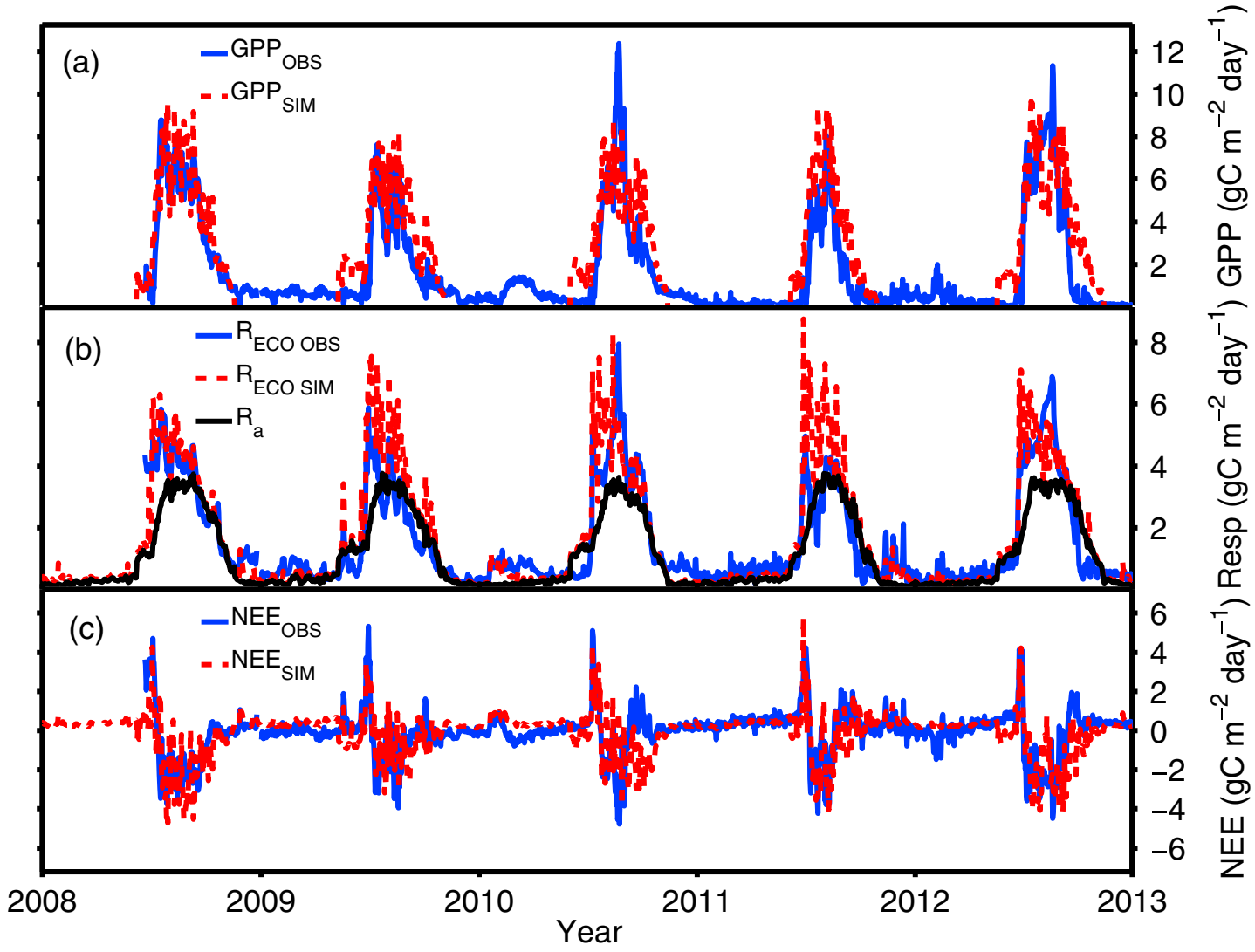

Figure 5. Comparison of observed (OBS) versus simulated (SIM) of (a) gross primary productivity (GPP), (b) ecosystem respiration (R_{ECO}) along with simulated autotrophic respiration (R_a), and (c) net ecosystem exchange (NEE). Simulated R_{ECO} was obtained by combining R_a from the ecohydrological model tRIBS-VEGGIE and R_h from the soil carbon model.

the study period, similar to measured values in semiarid shrublands (e.g., Bolton, Smith, & Link, 1993; Cardoso et al., 2015; Cheng et al., 2015; Goberna et al., 2007). As expected, low amounts of R_h occur during the winter and spring and increase substantially after the first rainfall event during the NAM due to the available SWC and labile substrate, consistent with Verduzco et al. (2015) and Zhang et al. (2014). Simulated litter decomposition decreased as the labile substrate amounts were depleted which leads to a reduction in the microbial biomass pool, similar to observations made in long-term incubation studies (Follett et al., 2007; Steinweg et al., 2008). As a result, the heterotrophic respiration was highly sensitive to the arrival of early storms during the NAM warm season, through its impact on SWC, and to the amount of labile substrate from the previous summer season, via the litterfall occurring at the end of the prior NAM.

By capturing R_h in the SCM, the simulated ecosystem respiration ($R_{ECO} = R_a + R_h$) was compared to EC measurements in Figure 5. Table 4 indicates a good correspondence between the observed and simulated R_{ECO} (CC $>$ 0.73, B within 0.09 of unity, MAE $<$ 0.04 g C m^{-2}) at hourly and daily resolutions. However, we noted discrepancies in the R_{ECO} for summers with high LAI, suggesting that autotrophic respiration (R_a) for plant growth and maintenance was overestimated to some extent. In addition, simulated R_{ECO} appeared flashier than the observations at the start of the summer season (Figure 5b) due to rapid changes in R_h

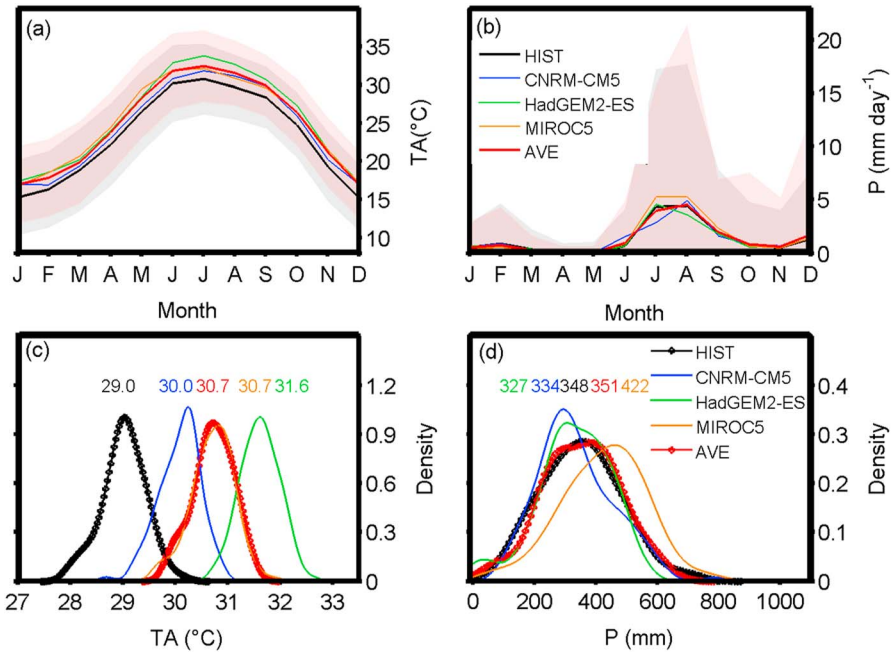

Figure 6. Comparison of meteorological conditions for historical (1990–2005) and climate change experiments (2030–2045) at the study site using representative realizations for HIST, CNRM-CM5, HadGEM2-ES, MIROC5, and AVE. (a, b) Monthly averages of daily air temperature (TA) and precipitation (*P*) with ±1 standard deviation shown as a shaded envelope for HIST (gray) and AVE (pink). (c, d) Probability density functions of summer (May-June-July-August-September, MJJAS) average TA and total *P*. Numbers indicate mean values for each case.

when both labile substrate and water were available and soil temperatures are high. As expected, the contribution of R_h to R_{ECO} decreased while the contribution of R_a increased during the temporal progression of the NAM season, reflecting the reduced role of microbial decomposition and the increased role of plant respiration during the growing period (e.g., Carbone et al., 2016).

Figure 5 and Table 4 also compare observed and simulated GPP, NEE, and NEP, respectively, indicating a reasonable match at hourly and daily scales. Note that the positive NEE (carbon loss) occurring early in the summer would not have been possible to represent without simulating R_h in the SCM, consistent with the metabolic activity of microbial communities when high quality litter inputs were available (Carbone et al., 2011; McCulley et al., 2004; Sponseller, 2007; Thiessen et al., 2013; Unger et al., 2010). Furthermore, the negative NEE (carbon uptake) during the growing season and the stable values of NEE near 0 during the dormant period were accurately captured by the models. Some issues are noted in 2010 which has an observed positive NEE in the late summer season that is not reproduced by the models. Nevertheless, similar patterns of annual NEP were found in the simulations and observations. During the study period, the subtropical shrubland acted as a net sink of carbon during most years (annual NEP from 33 to 105 g C m^{-2}), with the exception of 2011, in which both the simulations and observations indicated a net source of carbon (NEP of −53.1 and −98.3 g C m^{-2}).

3.2. Meteorological Changes in Historical and Climate Change Experiments

Figure 6 presents the outcomes of the stochastic downscaling procedure applied to historical (1990–2005, NLDAS) and near-future (2030–2045, CNRM-CM5, HadGEM2-ES, MIROC5, and AVE) periods in terms of the seasonal (monthly) cycle of TA and precipitation (Figures 6a and 6b) and the probability density functions (PDFs) of summertime TA and *P* (Figures 6c and 6d). These metrics were selected to show the range of meteorological changes in the experiments and summarize the model forcing tailored to the study site (i.e., a full set of hourly variables of 100 year duration for each scenario). Due to the model performance and the nature of the seasonal dynamics, a focus is placed on the summer season (May-June-July-August-September, MJJAS) in the analyses, including a distinction between premonsoon (May-June, MJ) and monsoon (July-August-September, JAS) periods. As expected from the RCP8.5 emissions case, a strong warming signal is present in the near future, with increases in mean annual temperature ranging from +1.1 to +2.3°C with respect to the HIST scenario. HadGEM2-ES exhibited the largest increase in mean summer TA

(+2.6°C), whereas CNRM-CM5 had the lowest increase (+1.0°C) relative to HIST. When averaged over the three models, the AVE scenario indicates a warming of +1.7°C in mean summer TA and a shift from a range of 24.4 to 33.6°C in HIST (±1 standard deviation envelop) to 26.1 to 35.3°C in AVE (Figure 6a). These effects are illustrated nicely through the PDFs of summer (MJJAS) average TA, obtained from hourly values over the 100 year sample size (Figure 6c). Note the increase in summer TA relative to HIST in the following order: CNRM-CM5, MIROC5, and HadGEM2-ES. These estimates are consistent with projections for the NAM (Cook & Seager, 2013; Lee & Wang, 2014; Maloney et al., 2014; Pachauri et al., 2014) suggesting a warming signal of +1.4 and 2.7°C between 2035 and 2065.

A comparison of the seasonal cycle of precipitation from the scenarios (Figure 6b) indicates that the use of factors of change in the stochastic downscaling method preserves rainfall seasonality as compared to the historical period with 60 to 80% of the annual precipitation occurring during summer (MJJAS), while leading to the differences in mean summer precipitation amounts (Figure 6d). Among the GCMs, HadGEM2-ES had lowest mean summer precipitation in the near-future period (327 mm or −21 mm with respect to HIST), whereas MIROC5 exhibited the highest mean summer *P* (422 mm or +74 mm relative to HIST). When averaged over the three models, the AVE scenario had a nearly identical mean monthly variation of *P* as HIST (Figure 6b), with a slightly expanded range of variability in August and October and a similar distribution of summer total *P* (Figure 6d). These comparisons are important since relative precipitation differences among GCMs (i.e., two GCMs have lower *P* and one has a higher *P* as compared to HIST) were quite larger than their temperature variations (i.e., all GCMs show rising TA). Precipitation variations in the scenarios might differ from other analysis of the CMIP5 models (Cook & Seager, 2013) or other downscaling approaches applied to the NAM region (Castro et al., 2012; Cerezo-Mota et al., 2011) since the historical seasonality at a monthly resolution was explicitly preserved, rather than allowed to evolve dynamically in the stochastic downscaling approach applied (Fatichi et al., 2013). Nevertheless, the considered scenarios captured a range of plausible near-future precipitation conditions, including increasing, decreasing, or no net change in summer amounts, under a warming trend that is considered realistic for the purposes of identifying climate change impacts.

3.3. Meteorological Change Effects on Simulated Water, Energy, and Carbon Dynamics

Responses to meteorological variations imposed by the climate change experiments were assessed first in the absence of increases in atmospheric CO_2 (365 ppm during 1990–2005). Figure 7 shows the results of the various scenarios (HIST, CNRM-CM5, HadGEM2-ES, MIROC5, and AVE) in terms of the monthly averaged SWC, ET, GPP, and NEP (Figures 7a–7d) during the summer period (MJJAS) as well as the probability density functions of summer season values (Figures 7e–7h), selected to illustrate the rich set of ecohydrological outcomes. The monthly values are obtained as averages over the 100 year periods, while the probability density functions show the full range of total summer season outcomes from each scenario and thus indicate interannual variability represented for historical and near-future conditions. The imposed TA and precipitation changes resulted in substantial summertime variations in the water, energy, and carbon dynamics among the climate change experiments. For instance, scenarios with summer precipitation lower than HIST (HadGEM2-ES and CNRM-CM5, Figure 6d) exhibited decreases in SWC (Figures 7a and 7e) and ET (Figures 7b and 7f), whereas scenarios with summer *P* at or above HIST (AVE and MIROC5) showed SWC and ET that were similar to or higher than HIST.

The strong correspondence between summer ET and SWC across simulations ($R^2 > 0.88, p < 0.05$) is typical of seasonally dry ecosystems (e.g., Scott et al., 2010; Vivoni et al., 2008). Nevertheless, TA differences among the climate change experiments also influenced ET through the sensitivity of plant physiological activity to warming. Specifically, stomatal conductance (g_s) in the simulations was reduced with rising TA for a constant CO_2 value due to increasing vapor pressure deficit and reductions on SWC (Verduzco, 2016). As an example, the HadGEM2-ES scenario with the highest TA (Figure 6c) exhibited increased evaporative demand, which causes complete vegetation failure leading to a reduction in ET due to elimination of the transpiration component. This is consistent with field studies in semiarid ecosystems reporting decreased stomatal conductance and carbon assimilation under warming-induced stress (Hamerlynck et al., 2000; Hamerlynck & Knapp, 1996; Ogle & Reynolds, 2002; Serrat-Capdevila et al., 2011).

Interestingly, differences among the climate change experiments were more pronounced when comparing carbon dynamics through the monthly evolution and summer total GPP (Figures 7c and 7g) and NEP (Figures 7d and 7h). This can be explained through the compensating effects of rising TA and changing *P*

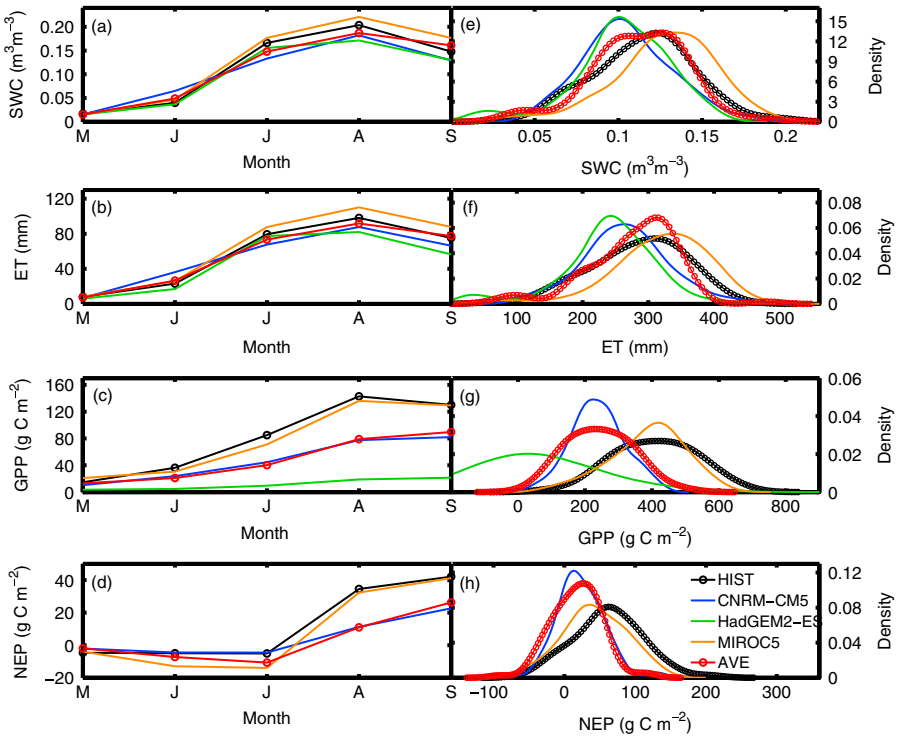

Figure 7. Comparison of water, energy, and carbon dynamics for historical (1990–2005) and climate change experiments (2030–2045) using representative realizations for HIST, CNRM-CM5, HadGEM2-ES, MIROC5, and AVE. Monthly mean values and seasonal probability density functions of (a, e) soil water content (SWC), (b, f) evapotranspiration (ET), (c, g) gross primary productivity (GPP), and (d, h) net ecosystem productivity (NEP) during summer (May-June-July-August-September, MJJAS).

on plant productivity and ecosystem respiration. For instance, MIROC5 and AVE exhibit similar values of TA that were both larger than HIST (Figure 6c), but there is a larger summer *P* in MIROC5 as compared to both AVE and HIST (which have similar totals, Figure 6d). While rising TA increases evaporative demand, higher *P* reduces soil moisture stress. The net result is an increase in GPP and NEP in MIROC5 relative to AVE, whereas MIROC5 and HIST are fairly close with respect to summer season carbon fluxes. This suggests that higher summer *P* has the capacity to compensate for increased summer TA (MIROC5 versus HIST), while maintaining similar precipitation under rising temperature leads to a lower GPP and NEP (AVE versus HIST). This latter case is consistent with experimental studies where increased temperatures have been shown to unfavorably affect productivity under constant precipitation treatments (e.g., Epstein et al., 1997; Mowll et al., 2015; Wu et al., 2011). Moreover, large increases in TA along with decreases in *P*, like the HadGEM2-ES scenario, significantly decrease GPP in the subtropical shrubland such that there is a collapse in the simulated plant activity. As a result, increased summertime TAs and reduced precipitation could cause large impacts on vegetation productivity that would require further plant adaptations or variations in community composition, as suggested in prior work (Dieleman et al., 2015; Goyal, 2004; Lavee et al., 1998; Moritz & Agudo, 2013; Ponce-Campos et al., 2013; Schwinning & Ehleringer, 2001).

A closer inspection of the summer carbon fluxes in Figure 8 reveals substantial variations between premonsoon (MJ) and monsoon (JAS) periods in the scenarios (HadGEM2-ES is omitted as GPP approached 0 after 35 years of simulation) as well as the relative importance of heterotrophic (R_h) and ecosystem respiration (R_{ECO}) on net ecosystem productivity. For all scenarios, premonsoon magnitudes of R_h and R_{ECO} were smaller than respiration fluxes during the monsoon, consistent with the drier soil conditions and lower microbial biomass (Figures 8a and 8b), as presented in other sites in the NAM region (Barron-Gafford et al., 2012). Furthermore, R_h is a larger fraction of R_{ECO} for the premonsoon period (R_h/R_{ECO} = 0.53, 0.52, 0.51 and 0.55 for HIST, CNRM-CM5, MIROC5, and AVE) as compared to monsoon conditions (R_h/R_{ECO} = 0.32, 0.31, 0.33, and 0.34), indicating that R_a increases in importance during the summer. Variations in monsoon values of respiration fluxes across the scenarios follow patterns in GPP (Figure 7g), as shown in prior studies (Gomez-Casanovas et al., 2012; Stoy et al., 2009). For example, R_h was correlated well with GPP ($R^2 > 0.60$, $p < 0.05$) such that scenarios with a

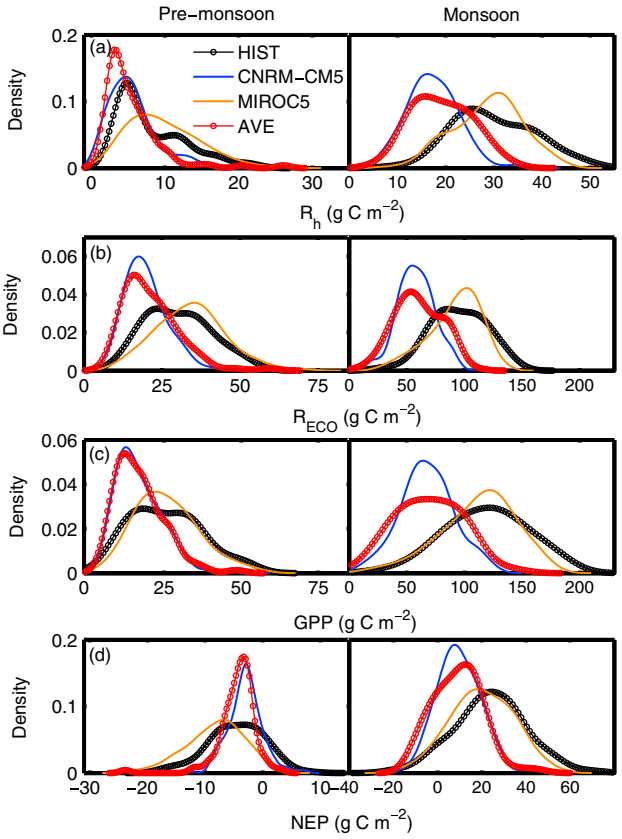

Figure 8. Comparison of carbon dynamics for historical (1990–2005) and climate change experiments (2030–2045) using representative realizations for HIST, CNRM-CM5, MIROC5, and AVE for premonsoon (May-June) and monsoon (July-August-September]) periods. Probability density functions of (a) heterotrophic respiration (R_h), (b) ecosystem respiration (R_{ECO}), (c) gross primary productivity (GPP), and (d) net ecosystem productivity (NEP) totals during each period.

higher GPP (HIST and MIROC5) exhibit higher R_h due to the increased availability of litterfall for decomposition (Figures 8b and 8c). In contrast, premonsoon periods showed sensitivity to both GPP and SWC such that MIROC5 with a higher *P* had substantially larger R_h than those scenarios with similar TA but lower *P*. This is consistent with other studies indicating that productivity enhancements via water availability are more critical controls on respiration than TA changes in semiarid ecosystems (Janssens et al., 2001; Reichstein et al., 2003). Premonsoon conditions also had substantially lower GPP and NEP as compared to the monsoon period (Figures 8c and 8d), with more negative values of NEP indicating the relative importance of R_{ECO} as compared to GPP prior to the growing season. Furthermore, higher precipitation and rising TAs (MIROC5) promote a more substantial R_h that reduce NEP, whereas a lower *P* and higher TA (CNRM-CM5 and AVE) resulted in NEP closer to 0. As a result, subtropical shrublands could become a larger net carbon source during premonsoon periods when warming is coupled with increased precipitation.

3.4. CO_2 Fertilization Effects on Simulated Water, Energy, and Carbon Dynamics

Superimposed effects of meteorological changes and increased atmospheric CO_2 concentrations (482 ppm over the 2030–2045 period) were assessed using a second set of simulations for each model scenario (CNRM-CM5, HadGEM2-ES, MIROC5, and AVE). Figure 9 presents the modeling outcomes for the climate change experiments (with and without CO_2 fertilization) relative to the HIST (1990–2005) simulation and the summer (MJJAS) averaged observations (OBS, 2008–2012). Differences between HIST and OBS were only due to the sampling of different time periods since simulations during 2008–2012 were consistent with OBS (Table 4). For the higher CO_2 scenarios, both GPP (+172.1, 188.5, and 210.5 g C m^{-2} for CNRM-CM5, MIROC5, and AVE, respectively) and R_{ECO} (+146.9, 147.0, and 153.7 g C m^{-2}) show increases when compared to the CO_2 of 365 ppm case (Figures 9a and 9b). Thus, for the same set of imposed meteorological changes, increased atmospheric CO_2 enhances GPP, as seen in field and remote sensing studies (Ainsworth & Long, 2005; Donohue et al., 2013; Morgan et al., 2004; Wang et al., 2012), and that is consistent with higher observed ecosystem respiration. Larger enhancements in GPP and R_{ECO} were noted for scenarios with more precipitation during the summer (MIROC5 versus CNRM-CM5). However, the increase in GPP due to CO_2 fertilization exceeds that of R_{ECO} due to a reduction of the autotrophic respiration per unit leaf area (e.g., Drake et al., 1997). As a result, NEP from the CO_2 fertilization experiments increased in terms of the median value and the range of values in all scenarios relative to simulations without a rising CO_2 (Figure 9c). Thus, CO_2 fertilization offsets the meteorological impacts on NEP in the near future (2030–2045) at the expense of an increase summer interannual variability. The positive effects of fertilization on the median NEP varied across the scenarios (+34.6, 33.2, and 33.9 g C m^{-2}) with a higher increase for AVE with the largest increase in WUE. In addition, the CO_2 fertilization altered NEP at the subtropical shrubland under the HadGEM2-ES scenario permitting ecosystem resilience and a positive carbon balance.

The role of precipitation changes on enhancing NEP was further explored by comparing SWC for the two sets of CO_2 experiments. As expected, higher GPP for scenarios with CO_2 fertilization was linked to a dramatic increase in LAI (+72%, 45%, and 73% for CNRM-CM5, MIROC5, and AVE, respectively) relative to the cases with CO_2 at 365 ppm, which resulted in a higher summertime ET (+18, 13, and 21 mm). While the higher ET under CO_2 fertilization would be expected to deplete soil water, we found no appreciable changes in SWC of the top 10 cm of soil (+0.0013, 0.0007, and 0.0019 m^3/m^3), even for cases where summertime precipitation decreased or remained similar (CNRM-CM5 and AVE). These results are consistent with Fatichi, Leuzinger, et al. (2016) who showed that increased WUE supports a higher LAI through soil

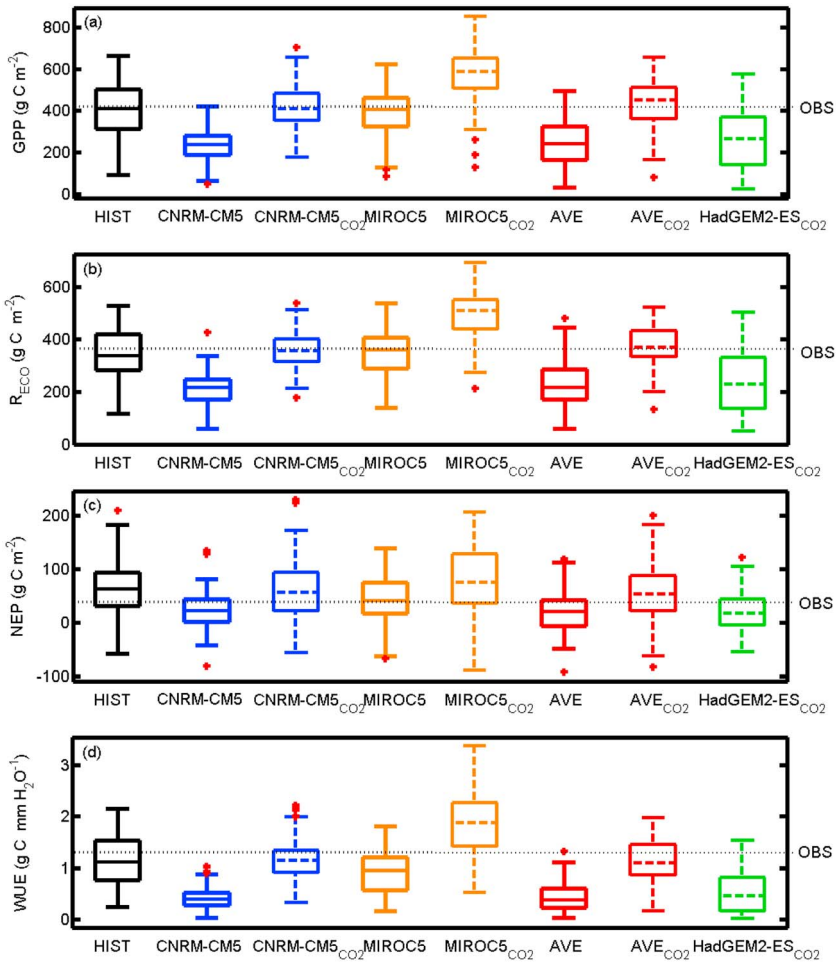

Figure 9. Box-whisker plots of summer (May-June-July-August-September) ecosystem respiration (R_{ECO}), gross primary productivity (GPP), net ecosystem productivity (NEP), and water use efficiency (WUE) for the climate change experiments under meteorological changes and superimposed CO_2 fertilization (labeled with subscript CO_2) using representative realizations for HIST, CNRM-CM5, HadGEM2-ES, MIROC5, and AVE. Dashed horizontal line in each subplot represents summer averages from observations (OBS, 2008–2012).

water savings but leads to a more rapid consumption of SWC due to the increased vegetation. The effects of increased CO_2 on gains in NEP despite a similar SWC when compared to scenarios without fertilization is attributed to ecosystem alterations in water use efficiency (WUE = GPP/ET, Figure 9d), which increased substantially (+68%, 42%, and 69%) at the expense of higher summertime interannual variability. Thus, a secondary effect of CO_2 fertilization is to allow more productive summers (i.e., higher NEP), when precipitation is not limiting, through higher WUE. As a result, CO_2 fertilization leads to a more efficient but variable ecosystem in terms of biomass production per amount of water consumed in most of the scenarios. Prior investigations have identified similar CO_2 fertilization effects on WUE, including through experimental studies of semiarid plants (e.g., Leakey et al., 2009; Morgan et al., 2011; Xu et al., 2014) and analyses of remotely sensed data in drylands (e.g., Donohue et al., 2013; Lu et al., 2016). Nevertheless, it has been uncommon to measure WUE directly in semiarid regions with strong vegetation dynamics. As such, there is a need to conduct additional observational analyses in seasonally dry ecosystems to compare with our model-based estimates of the CO_2 fertilization effect on WUE (+40% to 70%), as have been performed in temperate forests (Kauwe et al., 2013). In our study, the increase in WUE was greater in the warmest scenario (HadGEM2-ES) since elevated CO_2 allows plants to decrease stomatal conductance, while maintaining photosynthetic rates (Blumenthal et al., 2013), which resulted in positive NEP under CO_2 fertilization. Similar effects have been observed under experimental CO_2 fertilization (e.g., Cernusak et al., 2013; Conley et al., 2001) and more recently as a trend due to rising CO_2 concentrations (e.g., Lu et al., 2016; Maseyk et al., 2011).

4. Summary and Conclusions

In this work, we combined ecohydrological and soil carbon models to simulate water, energy, and carbon dynamics in a seasonally dry, semiarid ecosystem of northwestern México across temporal resolutions ranging from hourly to interannual variability. Compared to a set of field and remotely sensed observations, the tRIBS-VEGGIE and SCM simulations accurately captured the seasonality of vegetation activity and carbon fluxes of subtropical shrublands (Méndez-Barroso et al., 2014; Villarreal et al., 2016; Vivoni, Rodríguez, et al., 2010). In addition, the simulations represent the main features of net primary productivity in the region, specifically a large respiration pulse early in the summer followed by a gradual switch to carbon fixation during the growing season (Huxman et al., 2004; Verduzco et al., 2015; Yépez et al., 2007). This indicated that the simulation of soil (heterotrophic) respiration is an essential component for reproducing the observed carbon dynamics in this type of ecosystem. Furthermore, simulated R_h was highly sensitive to timing of the first storms during the NAM that increase SWC and to the amount of labile substrate derived from litterfall from the previous summer. Insights gained from the ecohydrological and soil carbon model application could potentially serve to improve terrestrial biosphere models (e.g., Huntzinger et al., 2012) that have been shown to misrepresent carbon dynamics in semiarid shrublands. Nevertheless, the use of the combined models within this ecosystem could be improved by adding a plant functional type, such as winter annuals (Werk et al., 1983) or evergreen shrubs (Biederman et al., 2018), that is active from fall to spring. In this manner, the physiological activity during winters would enhance the representation of vegetation dynamics and impact the generation and decomposition of litterfall, thus affecting the respiratory efflux at the start of the following monsoon. This is consistent with Verduzco et al. (2015) and Zhang et al. (2014), who suggested that the net carbon balance depends on the relative strength of the heterotrophic carbon release versus the primary productivity occurring later in the growing season. Overall, both the observed record and simulations over the studied (2008–2012) and historical (1990–2005) periods showed that the subtropical shrubland was generally a net carbon sink (positive NEP) over both growing season and annual time scales.

Subsequently, we conducted a comparison of historical (1990–2005) and near-future (2030–2045) climate change scenarios obtained from the stochastic downscaling of three GCMs (Fatichi et al., 2011, 2013) tailored for input to the tRIBS-VEGGIE and SCM models. Increased near-future TAs reduced net ecosystem productivity, though a compensation effect was identified for some of GCMs (e.g., MIROC5) exhibiting higher summer precipitation as compared to the historical scenario (HIST). This was attributed to higher plant stress under warmer temperatures and lower precipitation, which limited GPP. Since R_{ECO} was reduced to a lesser degree than GPP, due to warmer temperatures and short-term substrate availability, a lower NEP resulted in all scenarios, with compensation occurring when atmospheric CO_2 concentration was increased. When GCM projections of summer precipitation were substantially lower (HadGEM2-ES), a collapse of the simulated plant activity was observed (i.e., GPP approaching 0). It should be noted, however, that tRIBS-VEGGIE simulations do not currently account for plant thermal acclimation that can prevent "diebacks" due to high temperatures (Hamerlynck et al., 2000; Salvucci & Crafts-Brandner, 2004) or for plant mortality processes induced by cavitation (Fatichi, Pappas, et al., 2016; Plaut et al., 2012), and thus the collapse of plant activity under the HadGEM2-ES scenario is subject to considerable uncertainty.

Our main finding was that reductions in NEP under near-future meteorological changes were significantly offset under the CO_2 fertilization experiments for all considered GCMs. This was mainly attributed to an increase in WUE under elevated CO_2 concentrations via an indirect effect on SWC as identified in other water-limited ecosystems (Fatichi, Pappas, et al., 2016; Lu et al., 2016). As a result of higher SWC, the effects of warming-induced stress can be offset, leading to increases in NEP in the near future for all GCMs relative to the historical period. Increases in WUE under CO_2 fertilization help to explain how seasonally dry ecosystems can recover as a net carbon sink with a strength similar to the historical conditions under the superimposed climate change effects. For the scenario with higher summer precipitation (MIROC5), near-future NEP is larger than HIST, whereas for the case with the highest summer temperature (HadGEM2-ES), CO_2 fertilization prevents the collapse of the simulated plant activity. Nevertheless, these projected changes are also subject to uncertainty since photosynthetic acclimation to elevated CO_2 (Mueller et al., 2016; Newingham et al., 2013; Sage et al., 1989) is not currently considered.

Given the important role of semiarid regions in the terrestrial carbon budget (Ahlström et al., 2015; Poulter et al., 2014), the effects of meteorological changes and CO_2 fertilization on carbon dynamics in seasonally

dry ecosystems could have regional to global consequences. Under warming conditions, lower precipitation and increased atmospheric CO_2, our study suggests that semiarid ecosystems under the influence of the NAM would maintain a similar to actual net carbon balance by the mid-21st century. The offsetting of impacts from meteorological changes in temperature and precipitation and those arising from CO_2 fertilization is an outcome of opposing controls on soil and plant-mediated carbon dynamics. However, changes in the timing, intensity, and distribution of precipitation during the growing season (e.g., Cook & Seager, 2013; Geil et al., 2013), in particular an increase in monsoon rainfall (e.g., Hawkins et al., 2015; Robles-Morua et al., 2015), could lead to ecosystems acting as larger net carbon sinks, due to an increase in WUE under higher CO_2 concentrations, with implications on the global carbon budget. This outcome is consistent with observed biomass trends indicating more efficient productivity in semiarid ecosystems (Donohue et al., 2013), including those in the NAM region (Forzieri et al., 2014). While additional research is necessary to confirm the findings of this study and their implications for terrestrial biosphere models used to capture feedbacks to the climate system (Huntzinger et al., 2012), the combined use of dynamic ecosystem level measurements and numerical modeling is a promising avenue for deciphering the net effect of climate change on the water, energy, and carbon dynamics of seasonally dry, semiarid ecosystems.

Acknowledgments
We thank the Consejo Nacional de Ciencia y Tecnología (CONACYT) in México for the graduate fellowship to V. S. V. (231560) and T. T. (232184). This research project was supported by CB-2013-01: 221014 to E. A. Y. and a US Fulbright and CONACYT Visiting Fellowships to E. R. V. We also thank the World Climate Research Programme's Working Group on Coupled Modeling, for producing and making available the climate change model output. We thank two reviewers for excellent comments that helped to improve an earlier version of the manuscript. Data access is available through Zenodo at http://doi.org/10.5281/zenodo.1116422, and the model code and outputs utilized in this study can be requested from the corresponding author.

References

Ahlström, A., Raupach, M. R., Schurgers, G., Smith, B., Arneth, A., Jung, M., et al. (2015). The dominant role of semi-arid ecosystems in the trend and variability of the land CO_2 sink. *Science*, *348*(6237), 895–899. https://doi.org/10.1126/science.aaa1668

Ainsworth, E. A., & Long, S. P. (2005). What have we learned from 15 years of free-air CO_2 enrichment (FACE)? A meta-analytic review of the responses of photosynthesis, canopy properties and plant production to rising CO_2. *New Phytologist*, *165*(2), 351–372. https://doi.org/10.1111/j.1469-8137.2004.01224.x

Allard, V., Ourcival, J. M., Rambal, S., Joffre, R., & Rocheteau, A. (2008). Seasonal and annual variation of carbon exchange in an evergreen Mediterranean forest in southern France. *Global Change Biology*, *14*(4), 714–725. https://doi.org/10.1111/j.1365-2486.2008.01539.x

Amthor, J. S. (1984). The role of maintenance respiration in plant growth. *Plant, Cell & Environment*, *7*(8), 561–569. https://doi.org/10.1111/1365-3040.ep11591833

Anderson, C. A., & Vivoni, E. R. (2016). Impact of land surface states within the flux footprint on daytime land-atmosphere coupling in two semiarid ecosystems of the Southwestern US. *Water Resources Research*, *52*, 4785–4800. https://doi.org/10.1002/2015WR018016

Arnone, J. A. III, Verburg, P. S., Johnson, D. W., Larsen, J. D., Jasoni, R. L., Lucchesi, A. J., et al. (2008). Prolonged suppression of ecosystem carbon dioxide uptake after an anomalously warm year. *Nature*, *455*(7211), 383–386. https://doi.org/10.1038/nature07296

Aubinet, M., Grelle, A., Ibrom, A., Rannik, Ü., Moncrieff, J., Foken, T., et al. (2000). Estimates of the annual net carbon and water exchange of forests: The EUROFLUX methodology. *Advances in Ecological Research*, *30*, 113–175. https://doi.org/10.1016/S0065-2504(08)60018-5

Babst, F., Bouriaud, O., Papale, D., Gielen, B., Janssens, I. A., Nikinmaa, E., et al. (2014). Above-ground woody carbon sequestration measured from tree rings is coherent with net ecosystem productivity at five eddy-covariance sites. *New Phytologist*, *201*(4), 1289–1303. https://doi.org/10.1111/nph.12589

Baldocchi, D., Falge, E., Gu, L., Olson, R., Hollinger, D., Running, S., et al. (2001). FLUXNET: A new tool to study the temporal and spatial variability of ecosystem-scale carbon dioxide, water vapor, and energy flux densities. *Bulletin of the American Meteorological Society*, *82*(11), 2415–2434. https://doi.org/10.1175/1520-0477(2001)082%20%3C%202415:FANTTS%3E2.3.CO;2

Baldocchi, D. D. (2003). Assessing the eddy covariance technique for evaluating carbon dioxide exchange rates of ecosystems: Past, present and future. *Global Change Biology*, *9*(4), 479–492. https://doi.org/10.1046/j.1365-2486.2003.00629.x

Baldocchi, D. D. (2008). 'Breathing' of the terrestrial biosphere: Lessons learned from a global network of carbon dioxide flux measurement systems. *Australian Journal of Botany*, *56*(1), 1–26. https://doi.org/10.1071/BT07151

Barr, A. G., Richardson, A. D., Hollinger, D. Y., Papale, D., Arain, M. A., Black, T. A., et al. (2013). Use of change-point detection for friction-velocity threshold evaluation in eddy-covariance studies. *Agricultural and Forest Meteorology*, *171*, 31–45. https://doi.org/10.1016/j.agrformet.2012.11.023

Barron-Gafford, G. A., Scott, R. L., Jenerette, G. D., Hamerlynck, E. P., & Huxman, T. E. (2012). Temperature and precipitation controls over leaf- and ecosystem-level CO_2 flux along a woody plant encroachment gradient. *Global Change Biology*, *18*(4), 1389–1400. https://doi.org/10.1111/j.1365-2486.2011.02599.x

Biederman, J. A., Scott, R. L., Arnone, J., Jasoni, R. L., Litvak, M. E., Moreo, M. T., et al. (2018). Shrubland carbon sink depends upon winter water availability in the warm deserts of North America. *Agricultural and Forest Meteorology*, *249*, 407–419. https://doi.org/10.1016/j.agrformet.2017.11.005

Biederman, J. A., Scott, R. L., Bell, T., Bowling, D., Dore, S., Garatuza-Payan, J., et al. (2017). CO_2 exchange and evapotranspiration across dryland ecosystems of southwestern North America. *Global Change Biology*, *23*, 4204–4221. https://doi.org/10.1111/gcb.13686

Biederman, J. A., Scott, R. L., Goulden, M. L., Vargas, R., Litvak, M. E., Kolb, T. E., et al. (2016). Terrestrial carbon balance in a drier world: The effects of water availability in southwestern North America. *Global Change Biology*, *22*(5), 1867–1879. https://doi.org/10.1111/gcb.13222

Bisht, G. (2010). Satellite-based estimates of net radiation and modeling the role of topography and vegetation on inter-annual hydroclimatology, (Ph.D Thesis). Retrieved from http://hdl.handle.net/1721.1/60706. Massachusetts: Massachusetts Institute of Technology.

Blumenthal, D. M., Resco, V., Morgan, J. A., Williams, D. G., LeCain, D. R., Hardy, E. M., et al. (2013). Invasive forb benefits from water savings by native plants and carbon fertilization under elevated CO_2 and warming. *New Phytologist*, *200*(4), 1156–1165. https://doi.org/10.1111/nph.12459

Bolker, B. M., Pacala, S. W., & Parton, W. J. (1998). Linear analysis of soil decomposition: Insights from the century model. *Ecological Applications*, *8*(2), 425–439. https://doi.org/10.1890/1051-0761(1998)008%5B0425,LAOSDI%5D2.0.CO;2

Bolton, H., Smith, J. L., & Link, S. O. (1993). Soil microbial biomass and activity of a disturbed and undisturbed shrub-steppe ecosystem. *Soil Biology and Biochemistry*, *25*(5), 545–552. https://doi.org/10.1016/0038-0717(93)90192-E

Brown, DE (1994) Biotic communities: Southwestern United States and northwestern México. University of Utah Press, Salt Lake City, UT.
Búrquez, A., Martínez-Yrízar, A., & Núñez, S. (1999). Sonoran Desert productivity and the effect of trap size on litterfall estimates in dryland vegetation. *Journal of Arid Environments*, *43*(4), 459–465. https://doi.org/10.1006/jare.1999.0547
Cable, J. M., Ogle, K., Williams, D. G., Weltzin, J. F., & Huxman, T. E. (2008). Soil texture drives responses of soil respiration to precipitation pulses in the Sonoran Desert: Implications for climate change. *Ecosystems*, *11*(6), 961–979. https://doi.org/10.1007/s10021-008-9172-x
Carbone, M. S., Richardson, A. D., Chen, M., Davidson, E. A., Hughes, H., Savage, K. E., & Hollinger, D. Y. (2016). Constrained partitioning of autotrophic and heterotrophic respiration reduces model uncertainties of forest ecosystem carbon fluxes but not stocks. *Journal of Geophysical Research: Biogeosciences*, *121*, 2476–2492. https://doi.org/10.1002/2016JG003386
Carbone, M. S., Still, C. J., Ambrose, A. R., Dawson, T. E., Williams, A. P., Boot, C. M., et al. (2011). Seasonal and episodic moisture controls on plant and microbial contributions to soil respiration. *Oecologia*, *167*(1), 265–278. https://doi.org/10.1007/s00442-011-1975-3
Cardoso, J. A. F., Lima, A. M. N., Cunha, T. J. F., Rodrigues, M. S., Hernani, L. C., Amaral, A. J. D., & Oliveira Neto, M. B. D. (2015). Organic matter fractions in a quartzipsamment under cultivation of irrigated mango in the lower São Francisco valley region, Brazil. *Revista Brasileira de Ciência do Solo*, *39*(4), 1068–1078. https://doi.org/10.1590/01000683rbcs20140498
Castro, C. L., Chang, H. I., Dominguez, F., Carrillo, C., Schemm, J. K., & Henry Juang, H. M. (2012). Can a regional climate model improve the ability to forecast the North American monsoon? *Journal of Climate*, *25*(23), 8212–8237. https://doi.org/10.1175/JCLI-D-11-00441.1
Cerezo-Mota, R., Allen, M., & Jones, R. (2011). Mechanisms controlling precipitation in the northern portion of the North American monsoon. *Journal of Climate*, *24*(11), 2771–2783. https://doi.org/10.1175/2011JCLI3846.1
Cernusak, L. A., Winter, K., Dalling, J. W., Holtum, J. A., Jaramillo, C., Körner, C., et al. (2013). Tropical forest responses to increasing atmospheric CO_2: Current knowledge and opportunities for future research. *Functional Plant Biology*, *40*(6), 531–551. https://doi.org/10.1071/FP12309
Cheng, M., Xue, Z., Xiang, Y., Darboux, F., & An, S. (2015). Soil organic carbon sequestration in relation to revegetation on the Loess Plateau, China. *Plant and Soil*, *397*(1–2), 31–42. https://doi.org/10.1007/s11104-015-2486-5
Collins, S. L., Belnap, J., Grimm, N. B., Rudgers, J. A., Dahm, C. N., D'odorico, P., et al. (2014). A multiscale, hierarchical model of pulse dynamics in arid-land ecosystems. *Annual Review of Ecology, Evolution, and Systematics*, *45*, 397–419. https://doi.org/10.1146/annurev-ecolsys-120213-091650
Conant, R. T., Dalla-Betta, P., Klopatek, C. C., & Klopatek, J. M. (2004). Controls on soil respiration in semiarid soils. *Soil Biology and Biochemistry*, *36*(6), 945–951. https://doi.org/10.1016/j.soilbio.2004.02.013
Conley, M. M., Kimball, B. A., Brooks, T. J., Pinter, P. J., Hunsaker, D. J., Wall, G. W., et al. (2001). CO_2 enrichment increases water-use efficiency in sorghum. *New Phytologist*, *151*(2), 407–412. https://doi.org/10.1046/j.1469-8137.2001.00184.x
Cook, B. I., & Seager, R. (2013). The response of the North American Monsoon to increased greenhouse gas forcing. *Journal of Geophysical Research: Atmospheres*, *118*, 1690–1699. https://doi.org/10.1002/jgrd.50111
Davidson, E. A., Janssens, I. A., & Luo, Y. (2006). On the variability of respiration in terrestrial ecosystems: Moving beyond Q10. *Global Change Biology*, *12*(2), 154–164. https://doi.org/10.1111/j.1365-2486.2005.01065.x
Desai, A. R., Richardson, A. D., Moffat, A. M., Kattge, J., Hollinger, D. Y., Barr, A., et al. (2008). Cross-site evaluation of eddy covariance GPP and RE decomposition techniques. *Agricultural and Forest Meteorology*, *148*(6), 821–838. https://doi.org/10.1016/j.agrformet.2007.11.012
Dieleman, C. M., Branfireun, B. A., McLaughlin, J. W., & Lindo, Z. (2015). Climate change drives a shift in peatland ecosystem plant community: Implications for ecosystem function and stability. *Global Change Biology*, *21*(1), 388–395. https://doi.org/10.1111/gcb.12643
Donohue, R. J., Roderick, M. L., McVicar, T. R., & Farquhar, G. D. (2013). Impact of CO_2 fertilization on maximum foliage cover across the globe's warm, arid environments. *Geophysical Research Letters*, *40*, 3031–3035. https://doi.org/10.1002/grl.50563
Douglas, M. W., Maddox, R. A., Howard, K., & Reyes, S. (1993). The Mexican monsoon. *Journal of Climate*, *6*(8), 1665–1677. https://doi.org/10.1175/1520-0442(1993)006%3C1665:TMM%3E2.0.CO;2
Drake, B. G., Gonzàlez-Meler, M. A., & Long, S. P. (1997). More efficient plants: A consequence of rising atmospheric CO_2? *Annual Review of Plant Biology*, *48*(1), 609–639. https://doi.org/10.1146/annurev.arplant.48.1.609
Drake, J. E., Aspinwall, M. J., Pfautsch, S., Rymer, P. D., Reich, P. B., Smith, R. A., et al. (2015). The capacity to cope with climate warming declines from temperate to tropical latitudes in two widely distributed Eucalyptus species. *Global Change Biology*, *21*(1), 459–472. https://doi.org/10.1111/gcb.12729
Duan, Q. Y., Gupta, V. K., & Sorooshian, S. (1993). Shuffled complex evolution approach for effective and efficient global minimization. *Journal of Optimization Theory and Applications*, *76*, 501–521. https://doi.org/10.1007/BF00939380
Duarte, H. F., Dias, N. L., & Maggiotto, S. R. (2006). Assessing daytime downward longwave radiation estimates for clear and cloudy skies in Southern Brazil. *Agricultural and Forest Meteorology*, *139*(3), 171–181. https://doi.org/10.1016/j.agrformet.2006.06.008
Duursma, R. A., Barton, C. V. M., Lin, Y.-S., Medlyn, B. E., Eamus, D., Tissue, D. T., et al. (2014). The peaked response of transpiration rate to vapour pressure deficit in field conditions can be explained by the temperature optimum of photosynthesis. *Agricultural and Forest Meteorology*, *189–190*, 2–10. https://doi.org/10.1016/j.agrformet.2013.12.007
Epstein, H. E., Lauenroth, W. K., & Burke, I. C. (1997). Effects of temperature and soil texture on ANPP in the US Great Plains. *Ecology*, *78*(8), 2628–2631. https://doi.org/10.1890/0012-9658(1997)078%5B2628:EOTAST%5D2.0.CO;2
Euskirchen, E. S., Edgar, C. W., Turetsky, M. R., Waldrop, M. P., & Harden, J. W. (2014). Differential response of carbon fluxes to climate in three peatland ecosystems that vary in the presence and stability of permafrost. *Journal of Geophysical Research: Biogeosciences*, *119*, 1576–1595. https://doi.org/10.1002/2014JG002683
Fan, J., Jones, S. B., Qi, L. B., Wang, Q. J., & Huang, M. B. (2012). Effects of precipitation pulses on water and carbon dioxide fluxes in two semiarid ecosystems: Measurement and modeling. *Environmental Earth Sciences*, *67*(8), 2315–2324. https://doi.org/10.1007/s12665-012-1678-z
Fatichi, S., Ivanov, V. Y., & Caporali, E. (2011). Simulation of future climate scenarios with a weather generator. *Advances in Water Resources*, *34*(4), 448–467. https://doi.org/10.1016/j.advwatres.2010.12.013
Fatichi, S., Ivanov, V. Y., & Caporali, E. (2013). Assessment of a stochastic downscaling methodology in generating an ensemble of hourly future climate time series. *Climate Dynamics*, *40*(7–8), 1841–1861. https://doi.org/10.1007/s00382-012-1627-2
Fatichi, S., Leuzinger, S., Paschalis, A., Langley, J. A., Barraclough, A. D., & Hovenden, M. J. (2016). Partitioning direct and indirect effects reveals the response of water-limited ecosystems to elevated CO_2. *Proceedings of the National Academy of Sciences*, *113*(45), 12,757–12,762. https://doi.org/10.1073/pnas.1605036113
Fatichi, S., Pappas, C., & Ivanov, V. Y. (2016). Modeling plant–water interactions: An ecohydrological overview from the cell to the global scale. *Wiley Interdisciplinary Reviews: Water*, *3*(3), 327–368. https://doi.org/10.1002/wat2.1125
Fensholt, R., Sandholt, I., & Rasmussen, M. S. (2004). Evaluation of MODIS LAI, fAPAR and the relation between fAPAR and NDVI in a semi-arid environment using in situ measurements. *Remote Sensing of Environment*, *91*(3), 490–507. https://doi.org/10.1016/j.rse.2004.04.009
Fisher, J. B., Huntzinger, D. N., Schwalm, C. R., & Sitch, S. (2014). Modeling the terrestrial biosphere. *Annual Review of Environment and Resources*, *39*, 91–123. https://doi.org/10.1146/annurev-environ-012913-093456

Flanagan, L. B., Wever, L. A., & Carlson, P. J. (2002). Seasonal and interannual variation in carbon dioxide exchange and carbon balance in a northern temperate grassland. *Global Change Biology*, *8*(7), 599–615. https://doi.org/10.1046/j.1365-2486.2002.00491.x

Flato, G., Marotzke, J., Abiodun, B., Braconnot, P., Chou, S. C., Collins, W. J., et al. (2013). Evaluation of climate models. In: Climate change 2013: The physical science basis. Contribution of Working Group I to the fifth assessment report of the Intergovernmental Panel on Climate Change. *Climate Change 2013*, *5*, 741–866. https://doi.org/10.1017/CBO9781107415324.020

Follett, R. F., Paul, E. A., & Pruessner, E. G. (2007). Soil carbon dynamics during a long-term incubation study involving ^{13}C and ^{14}C measurements. *Soil Science*, *172*(3), 189–208. https://doi.org/10.1097/ss.0b013e31803403de

Forzieri, G., Feyen, L., Cescatti, A., & Vivoni, E. R. (2014). Spatial and temporal variations in ecosystem response to monsoon precipitation variability in southwestern North America. *Journal of Geophysical Research: Biogeosciences*, *119*, 1999–2017. https://doi.org/10.1002/2014JG002710

Friedlingstein, P., Meinshausen, M., Arora, V. K., Jones, C. D., Anav, A., Liddicoat, S. K., & Knutti, R. (2014). Uncertainties in CMIP5 climate projections due to carbon cycle feedbacks. *Journal of Climate*, *27*(2), 511–526. https://doi.org/10.1175/JCLI-D-12-00579.1

Geil, K. L., Serra, Y. L., & Zeng, X. (2013). Assessment of CMIP5 model simulations of the North American monsoon system. *Journal of Climate*, *26*(22), 8787–8801. https://doi.org/10.1175/JCLI-D-13-00044.1

Gherardi, L. A., & Sala, O. E. (2015). Enhanced precipitation variability decreases grass-and increases shrub-productivity. *Proceedings of the National Academy of Sciences*, *112*(41), 12,735–12,740. https://doi.org/10.1073/pnas.1506433112

Goberna, M., Pascual, J. A., Garcia, C., & Sánchez, J. (2007). Do plant clumps constitute microbial hotspots in semiarid Mediterranean patchy landscapes? *Soil Biology and Biochemistry*, *39*(5), 1047–1054. https://doi.org/10.1016/j.soilbio.2006.11.015

Gomez-Casanovas, N., Matamala, R., Cook, D. R., & Gonzalez-Meler, M. A. (2012). Net ecosystem exchange modifies the relationship between the autotrophic and heterotrophic components of soil respiration with abiotic factors in prairie grasslands. *Global Change Biology*, *18*(8), 2532–2545. https://doi.org/10.1111/j.1365-2486.2012.02721.x

Goyal, R. K. (2004). Sensitivity of evapotranspiration to global warming: A case study of arid zone of Rajasthan (India). *Agricultural Water Management*, *69*(1), 1–11. https://doi.org/10.1016/j.agwat.2004.03.014

Hamerlynck, E., & Knapp, A. K. (1996). Photosynthetic and stomatal responses to high temperature and light in two oaks at the western limit of their range. *Tree Physiology*, *16*(6), 557–565. https://doi.org/10.1093/treephys/16.6.557

Hamerlynck, E. P., Huxman, T. E., Loik, M. E., & Smith, S. D. (2000). Effects of extreme high temperature, drought and elevated CO_2 on photosynthesis of the Mojave Desert evergreen shrub, *Larrea tridentata*. *Plant Ecology*, *148*(2), 183–193.

Harper, C. W., Blair, J. M., Fay, P. A., Knapp, A. K., & Carlisle, J. D. (2005). Increased rainfall variability and reduced rainfall amount decreases soil CO_2 flux in a grassland ecosystem. *Global Change Biology*, *11*(2), 322–334. https://doi.org/10.1111/j.1365-2486.2005.00899.x

Hawkins, G. A., Vivoni, E. R., Robles-Morua, A., Mascaro, G., Rivera, E., & Dominguez, F. (2015). A climate change projection for summer hydrologic conditions in a semiarid watershed of central Arizona. *Journal of Arid Environments*, *118*, 9–20. https://doi.org/10.1016/j.jaridenv.2015.02.022

Heisler-White, J. L., Knapp, A. K., & Kelly, E. F. (2008). Increasing precipitation event size increases aboveground net primary productivity in a semi-arid grassland. *Oecologia*, *158*(1), 129–140. https://doi.org/10.1007/s00442-008-1116-9

Huntzinger, D. N., Post, W. M., Wei, Y., Michalak, A. M., West, T. O., Jacobson, A. R., et al. (2012). North American Carbon Program (NACP) regional interim synthesis: Terrestrial biospheric model intercomparison. *Ecological Modeling*, *232*, 144–157. https://doi.org/10.1016/j.ecolmodel.2012.02.004

Huxman, T. E., Snyder, K. A., Tissue, D., Leffler, A. J., Ogle, K., Pockman, W. T., et al. (2004). Precipitation pulses and carbon fluxes in semiarid and arid ecosystems. *Oecologia*, *141*(2), 254–268. https://doi.org/10.1007/s00442-004-1682-4

INEGI (2010). Conjunto Nacional de Uso de Suelo y Vegetación a escala 1:250,000, DGG-INEGI, México. Serie IV.

IPCC (2013). Climate change 2013: The physical science basis. In T. F. Stocker, et al. (Eds.), *Contribution of Working Group I to the fifth assessment report of the Intergovernmental Panel on Climate Change* (Chapter 8, pp. 659–740). Cambridge, United Kingdom and New York, NY, USA: Cambridge University Press. https://doi.org/10.1017/CBO9781107415324

Ivanov, V. Y., Bras, R. L., & Vivoni, E. R. (2008a). Vegetation-hydrology dynamics in complex terrain of semiarid areas: 1. A mechanistic approach to modeling dynamic feedbacks. *Water Resources Research*, *44*, W03429. https://doi.org/10.1029/2006WR005588

Ivanov, V. Y., Bras, R. L., & Vivoni, E. R. (2008b). Vegetation-hydrology dynamics in complex terrain of semiarid areas: 1. Energy-water controls of vegetation spatiotemporal dynamics and topographic niches of favorability. *Water Resources Research*, *44*, W03430. https://doi.org/10.1029/2006WR005595

Jackson, R. B., Canadell, J., Ehleringer, J. R., Mooney, H. A., Sala, O. E., & Schulze, E. D. (1996). A global analysis of root distributions for terrestrial biomes. *Oecologia*, *108*(3), 389–411. https://doi.org/10.1007/BF00333714

Janssens, I. A., Lankreijer, H., Matteucci, G., Kowalski, A. S., Buchmann, N., Epron, D., et al. (2001). Productivity overshadows temperature in determining soil and ecosystem respiration across European forests. *Global Change Biology*, *7*(3), 269–278. https://doi.org/10.1046/j.1365-2486.%202001.00412.x

Jenerette, G. D., Scott, R. L., & Huete, A. R. (2010). Functional differences between summer and winter season rain assessed with MODIS-derived phenology in a semi-arid region. *Journal of Vegetation Science*, *21*(1), 16–30. https://doi.org/10.1111/j.1654-1103.2009.01118.x

Kauwe, M. G., Medlyn, B. E., Zaehle, S., Walker, A. P., Dietze, M. C., Hickler, T., et al. (2013). Forest water use and water use efficiency at elevated CO_2: A model-data intercomparison at two contrasting temperate forest FACE sites. *Global Change Biology*, *19*(6), 1759–1779. https://doi.org/10.1111/gcb.12164

Keenan, T. F., Baker, I., Barr, A., Ciais, P., Davis, K., Dietze, M., et al. (2012). Terrestrial biosphere model performance for inter-annual variability of land-atmosphere CO_2 exchange. *Global Change Biology*, *18*(6), 1971–1987. https://doi.org/10.1111/j.1365-2486.2012.02678.x

Kunkel, K. E. (2016). Update to data originally published in: Kunkel, K.E., D.R. Easterling, K. Hubbard, and K. Redmond. 2004. Temporal variations in frost-free season in the United States: 1895–2000. *Geophysical Research Letters*, *31*, L03201. https://doi.org/10.1029/2003GL018624

Lavee, H., Imeson, A. C., & Sarah, P. (1998). The impact of climate change on geomorphology and desertification along a Mediterranean-arid transect. *Land Degradation & Development*, *9*(5), 407–422. https://doi.org/10.1002/(SICI)1099-145X(199809/10)9:5%20%3C%20407::AID-LDR302%20%3E%203.0.CO;2%E2%80%936

Leakey, A. D., Ainsworth, E. A., Bernacchi, C. J., Rogers, A., Long, S. P., & Ort, D. R. (2009). Elevated CO_2 effects on plant carbon, nitrogen, and water relations: Six important lessons from FACE. *Journal of Experimental Botany*, *60*(10), 2859–2876. https://doi.org/10.1093/jxb/erp096

Lee, J. Y., & Wang, B. (2014). Future change of global monsoon in the CMIP5. *Climate Dynamics*, *42*(1–2), 101–119. https://doi.org/10.1007/s00382-012-1564-0

Lenton, T. M., & Huntingford, C. (2003). Global terrestrial carbon storage and uncertainties in its temperature sensitivity examined with a simple model. *Global Change Biology*, *9*(10), 1333–1352. https://doi.org/10.1046/j.1365-2486.2003.00674.x

Li, T., Grant, R. F., & Flanagan, L. B. (2004). Climate impact on net ecosystem productivity of a semi-arid natural grassland: Modeling and measurement. *Agricultural and Forest Meteorology*, *126*(1), 99–116. https://doi.org/10.1016/j.agrformet.2004.06.005

Liu, W., Zhang, Z. H. E., & Wan, S. (2009). Predominant role of water in regulating soil and microbial respiration and their responses to climate change in a semiarid grassland. *Global Change Biology*, *15*(1), 184–195. https://doi.org/10.1111/j.1365-2486.2008.01728.x

Lloyd, J., & Taylor, J. A. (1994). On the temperature dependence of soil respiration. *Functional Ecology*, *8*(3), 315–323. https://doi.org/10.2307/2389824

Loescher, H. W., Oberbauer, S. F., Gholz, H. L., & Clark, D. B. (2003). Environmental controls on net ecosystem-level carbon exchange and productivity in a Central American tropical wet forest. *Global Change Biology*, *9*(3), 396–412. https://doi.org/10.1046/j.1365-2486.2003.00599.x

Lu, X., Wang, L., & McCabe, M. F. (2016). Elevated CO_2 as a driver of global dryland greening. *Scientific Reports*, *6*, 20,716. https://doi.org/10.1038/srep20716

Luo, Y., Wan, S., Hui, D., & Wallace, L. L. (2001). Acclimatization of soil respiration to warming in a tall grass prairie. *Nature*, *413*(6856), 622–625. https://doi.org/10.1038/35098065

Maloney, E. D., Camargo, S. J., Chang, E., Colle, B., Fu, R., Geil, K. L., et al. (2014). North American climate in CMIP5 experiments: Part III: Assessment of twenty-first-century projections. *Journal of Climate*, *27*(6), 2230–2270. https://doi.org/10.1175/JCLI-D-13-00273.1

Manzoni, S., Porporato, A., D'Odorico, P., Laio, F., & Rodriguez-Iturbe, I. (2004). Soil nutrient cycles as a nonlinear dynamical system. *Nonlinear Processes in Geophysics*, *11*(5/6), 589–598.

Martínez-Yrízar, A., Núñez, S., & Burquez, A. (2007). Leaf litter decomposition in a southern Sonoran Desert ecosystem, northwestern Mexico: Effects of habitat and litter quality. *Acta Oecologica*, *32*(3), 291–300. https://doi.org/10.1016/j.actao.2007.05.010

Martínez-Yrízar, A., Núñez, S., Miranda, H., & Búrquez, A. (1999). Temporal and spatial variation of litter production in Sonoran Desert communities. *Plant Ecology*, *145*(1), 37–48. https://doi.org/10.1023/A:1009896201047

Maseyk, K., Hemming, D., Angert, A., Leavitt, S. W., & Yakir, D. (2011). Increase in water-use efficiency and underlying processes in pine forests across a precipitation gradient in the dry Mediterranean region over the past 30 years. *Oecologia*, *167*(2), 573–585. https://doi.org/10.1007/s00442-011-2010-4

Massman, W. J. (2001). Reply to comment by Rannik on: "A simple method for estimating frequency response corrections for eddy covariance systems". *Agricultural and Forest Meteorology*, *107*, 247–251.

McCulley, R. L., Archer, S. R., Boutton, T. W., Hons, F. M., & Zuberer, D. A. (2004). Soil respiration and nutrient cycling in wooded communities developing in grassland. *Ecology*, *85*(10), 2804–2817. https://doi.org/10.1890/03-0645

Méndez-Barroso, L. A., Vivoni, E. R., Robles-Morua, A., Mascaro, G., Yépez, E. A., Rodríguez, J. C., et al. (2014). A modeling approach reveals differences in evapotranspiration and its partitioning in two semiarid ecosystems in Northwest Mexico. *Water Resources Research*, *50*, 3229–3252. https://doi.org/10.1002/2013WR014838

Méndez-Barroso, L. A., Vivoni, E. R., Watts, C. J., & Rodríguez, J. C. (2009). Seasonal and interannual relations between precipitation, surface soil moisture and vegetation dynamics in the North American monsoon region. *Journal of Hydrology*, *377*(1), 59–70. https://doi.org/10.1016/j.jhydrol.2009.08.009

Miranda, J. D. D., Armas, C., Padilla, F. M., & Pugnaire, F. I. (2011). Climatic change and rainfall patterns: Effects on semi-arid plant communities of the Iberian Southeast. *Journal of Arid Environments*, *75*(12), 1302–1309. https://doi.org/10.1016/j.jaridenv.2011.04.022

Mitchell, K. E., Lohmann, D., Houser, P. R., Wood, E. F., Schaake, J. C., Robock, A., et al. (2004). The multi-institution North American Land Data Assimilation System (NLDAS): Utilizing multiple GCIP products and partners in a continental distributed hydrological modeling system. *Journal of Geophysical Research*, *109*, D07S90. https://doi.org/10.1029/2003JD003823

Morgan, J. A., LeCain, D. R., Pendall, E., Blumenthal, D. M., Kimball, B. A., Carrillo, Y., et al. (2011). C4 grasses prosper as carbon dioxide eliminates desiccation in warmed semi-arid grassland. *Nature*, *476*(7359), 202–205. https://doi.org/10.1038/nature10274

Morgan, J. A., Mosier, A. R., Milchunas, D. G., LeCain, D. R., Nelson, J. A., & Parton, W. J. (2004). CO_2 enhances productivity of the shortgrass steppe, alters species composition, and reduces forage digestibility. *Ecological Applications*, *14*, 208–219.

Moritz, C., & Agudo, R. (2013). The future of species under climate change: Resilience or decline? *Science*, *341*(6145), 504–508. https://doi.org/10.1126/science.1237190

Mowll, W., Blumenthal, D. M., Cherwin, K., Smith, A., Symstad, A. J., Vermeire, L. T., et al. (2015). Climatic controls of aboveground net primary production in semi-arid grasslands along a latitudinal gradient portend low sensitivity to warming. *Oecologia*, *177*(4), 959–969. https://doi.org/10.1007/s0044

Mueller, K. E., Blumenthal, D. M., Pendall, E., Carrillo, Y., Dijkstra, F. A., Williams, D. G., et al. (2016). Impacts of warming and elevated CO_2 on a semi-arid grassland are non-additive, shift with precipitation, and reverse over time. *Ecology Letters*, *19*(8), 956–966. https://doi.org/10.1111/ele.12634

Nagol, J. R., Vermote, E. F., & Prince, S. D. (2009). Effects of atmospheric variation on AVHRR NDVI data. *Remote Sensing of Environment*, *113*(2), 392–397. https://doi.org/10.1016/j.rse.2008.10.007

Nayak, R. K., Patel, N. R., & Dadhwal, V. K. (2015). Spatio-temporal variability of net ecosystem productivity over India and its relationship to climatic variables. *Environmental Earth Sciences*, *74*(2), 1743–1753. https://doi.org/10.1007/s12665-015-4182-4

Newingham, B. A., Vanier, C. H., Charlet, T. N., Ogle, K., Smith, S. D., & Nowak, R. S. (2013). No cumulative effect of 10 years of elevated [CO_2] on perennial plant biomass components in the Mojave Desert. *Global Change Biology*, *19*(7), 2168–2181. https://doi.org/10.1111/gcb.12177

Novick, K. A., Ficklin, D. L., Stoy, P. C., Williams, C. A., Bohrer, G., Oishi, A. C., et al. (2016). The increasing importance of atmospheric demand for ecosystem water and carbon fluxes. *Nature Climate Change*, *6*(11), 1023–1027. https://doi.org/10.1038/nclimate3114

Núñez, S., Martínez-Yrízar, A., Búrquez, A., & García-Oliva, F. (2001). Carbon mineralization in the southern Sonoran Desert. *Acta Oecologica*, *22*(5), 269–276. https://doi.org/10.1016/S1146-609X(01)01122-5

Ogle, K., & Reynolds, J. F. (2002). Desert dogma revisited: Coupling of stomatal conductance and photosynthesis in the desert shrub, *Larrea tridentata*. *Plant, Cell & Environment*, *25*(7), 909–921. https://doi.org/10.1046/j.1365-3040.2002.00876.x

ORNL DAAC. 2008. MODIS Collection 5 land products global subsetting and visualization tool. ORNL DAAC, Oak Ridge, Tennessee, USA. Accessed January 18, 2017. doi:https://doi.org/10.3334/ORNLDAAC/1241

Pachauri, R. K., Allen, M. R., Barros, V. R., Broome, J., Cramer, W., Christ, R., & Dubash, N. K. (2014). Climate change 2014: Synthesis report. Contribution of Working Groups I, II and III to the fifth assessment report of the Intergovernmental Panel on Climate Change (p. 151). IPCC.

Parolari, A. J., & Porporato, A. (2016). Forest soil carbon and nitrogen cycles under biomass harvest: Stability, transient response, and feedback. *Ecological Modeling*, *329*, 64–76. https://doi.org/10.1016/j.ecolmodel.2016.03.003

Pavón, N. P., Briones, O., & Flores-Rivas, J. (2005). Litterfall production and nitrogen content in an intertropical semi-arid Mexican scrub. *Journal of Arid Environments*, *60*(1), 1–13. https://doi.org/10.1016/j.jaridenv.2004.03.004

Pérez-Ruiz, E. R., Garatuza-Payan, J., Watts, C. J., Rodriguez, J. C., Yepez, E. A., & Scott, R. L. (2010). Carbon dioxide and water vapor exchange in a tropical dry forest as influenced by the North American Monsoon System (NAMS). *Journal of Arid Environments*, *74*(5), 556–563. https://doi.org/10.1016/j.jaridenv.2009.09.029

Plaut, J. A., Yepez, E. A., Hill, J., Pangle, R., Sperry, J. S., Pockman, W. T., & Mcdowell, N. G. (2012). Hydraulic limits preceding mortality in a piñon–juniper woodland under experimental drought. *Plant, Cell & Environment*, *35*(9), 1601–1617. https://doi.org/10.1111/j.1365-3040.2012.02512.x

Ponce-Campos, G. E., Moran, M. S., Huete, A., Zhang, Y., Bresloff, C., Huxman, T. E., et al. (2013). Ecosystem resilience despite large-scale altered hydroclimatic conditions. *Nature*, *494*(7437), 349–352. https://doi.org/10.1038/nature11836

Porporato, A., D'odorico, P., Laio, F., & Rodriguez-Iturbe, I. (2003). Hydrologic controls on soil carbon and nitrogen cycles. I. Modeling scheme. *Advances in Water Resources*, *26*(1), 45–58. https://doi.org/10.1016/S0309-1708(02)00094-5

Poulter, B., Frank, D., Ciais, P., Myneni, R. B., Andela, N., Bi, J., et al. (2014). Contribution of semi-arid ecosystems to interannual variability of the global carbon cycle. *Nature*, *509*(7502), 600–603. https://doi.org/10.1038/nature13376

Rawls, W. J., Brakensiek, D. L., & Saxtonn, K. E. (1982). Estimation of soil water properties. *Transactions of ASAE*, *25*(5), 1316–1320. https://doi.org/10.13031/2013.33720

Reichstein, M., Falge, E., Baldocchi, D., Papale, D., Aubinet, M., Berbigier, P., et al. (2005). On the separation of net ecosystem exchange into assimilation and ecosystem respiration: Review and improved algorithm. *Global Change Biology*, *11*(9), 1424–1439. https://doi.org/10.1111/j.1365-2486.2005.001002.x

Reichstein, M., Rey, A., Freibauer, A., Tenhunen, J., Valentini, R., Banza, J., et al. (2003). Modeling temporal and large-scale spatial variability of soil respiration from soil water availability, temperature and vegetation productivity indices. *Global Biogeochemical Cycles*, *17*(4), 1104. https://doi.org/10.1029/2003GB002035

Robertson, T. R., Bell, C. W., Zak, J. C., & Tissue, D. T. (2009). Precipitation timing and magnitude differentially affect aboveground annual net primary productivity in three perennial species in a Chihuahuan Desert grassland. *New Phytologist*, *181*(1), 230–242. https://doi.org/10.1111/j.1469-8137.2008.02643.x

Robles-Morua, A., Che, D., Mayer, A. S., & Vivoni, E. R. (2015). Hydrological assessment of proposed reservoirs in the Sonora River Basin, Mexico, under historical and future climate scenarios. *Hydrological Sciences Journal*, *60*(1), 50–66. https://doi.org/10.1080/02626667.2013.878462

Robles-Morua, A., Vivoni, E. R., & Mayer, A. S. (2012). Distributed hydrologic modeling in northwest Mexico reveals the links between runoff mechanisms and evapotranspiration. *Journal of Hydrometeorology*, *13*(3), 785–807. https://doi.org/10.1175/JHM-D-11-0112.1

Rodríguez-Iturbe, I., & Porporato, A. (2004). *Ecohydrology of water-controlled ecosystems: Soil moisture and plant dynamics* (442 pp.). Cambridge, UK: Cambridge University Press.

Rohr, T., Manzoni, S., Feng, X., Menezes, R. S., & Porporato, A. (2013). Effect of rainfall seasonality on carbon storage in tropical dry ecosystems. *Journal of Geophysical Research: Biogeosciences*, *118*, 1156–1167. https://doi.org/10.1002/jgrg.20091

Ross, I., Misson, L., Rambal, S., Arneth, A., Scott, R. L., Carrara, A., et al. (2012). How do variations in the temporal distribution of rainfall events affect ecosystem fluxes in seasonally water-limited Northern Hemisphere shrublands and forests? *Biogeosciences*, *9*, 1007–1024. https://doi.org/10.5194/bg-9-1007-2012

Ryan, M. G. (1991). Effects of climate change on plant respiration. *Ecological Applications*, *1*(2), 157–167. https://doi.org/10.2307/1941808

Sacks, W. J., Schimel, D. S., & Monson, R. K. (2007). Coupling between carbon cycling and climate in a high-elevation, subalpine forest: A model-data fusion analysis. *Oecologia*, *151*(1), 54–68. https://doi.org/10.1007/s00442-006-0565-2

Sage, R. F., & Kubien, D. S. (2007). The temperature response of C_3 and C_4 photosynthesis. *Plant, Cell & Environment*, *30*(9), 1086–1106. https://doi.org/10.1111/j.1365-3040.2007.01682.x

Sage, R. F., Sharkey, T. D., & Seemann, J. R. (1989). Acclimation of photosynthesis to elevated CO_2 in five C_3 species. *Plant Physiology*, *89*(2), 590–596. https://doi.org/10.1104/pp.89.2.590

Salvucci, M. E., & Crafts-Brandner, S. J. (2004). Relationship between the heat tolerance of photosynthesis and the thermal stability of Rubisco activase in plants from contrasting thermal environments. *Plant Physiology*, *134*(4), 1460–1470. https://doi.org/10.1104/pp.103.038323

Schwinning, S., & Ehleringer, J. R. (2001). Water use trade-offs and optimal adaptations to pulse-driven arid ecosystems. *Journal of Ecology*, *89*(3), 464–480. https://doi.org/10.1046/j.1365-2745.2001.00576.x

Scott, R. L., Biederman, J. A., Hamerlynck, E. P., & Barron-Gafford, G. A. (2015). The carbon balance pivot point of southwestern US semiarid ecosystems: Insights from the 21st century drought. *Journal of Geophysical Research: Biogeosciences*, *120*, 2612–2624. https://doi.org/10.1002/2015JG003181

Scott, R. L., Edwards, E. A., Shuttleworth, W. J., Huxman, T. E., Watts, C., & Goodrich, D. C. (2004). Interannual and seasonal variation in fluxes of water and carbon dioxide from a riparian woodland ecosystem. *Agricultural and Forest Meteorology*, *122*(1), 65–84. https://doi.org/10.1016/j.agrformet.2003.09.001

Scott, R. L., Hamerlynck, E. P., Jenerette, G. D., Moran, M. S., & Barron-Gafford, G. A. (2010). Carbon dioxide exchange in a semidesert grassland through drought-induced vegetation change. *Journal of Geophysical Research: Biogeosciences*, *115*, G03026. https://doi.org/10.1029/2010JG001348

Seager, R., Ting, M., Held, I., Kushnir, Y., Lu, J., Vecchi, G., et al. (2007). Model projections of an imminent transition to a more arid climate in southwestern North America. *Science*, *316*(5828), 1181–1184. https://doi.org/10.1126/science.1139601

Seneviratne, S. I., Corti, T., Davin, E. L., Hirschi, M., Jaeger, E. B., Lehner, I., et al. (2010). Investigating soil moisture–climate interactions in a changing climate: A review. *Earth-Science Reviews*, *99*(3), 125–161. https://doi.org/10.1016/j.earscirev.2010.02.004

Serrat-Capdevila, A., Scott, R. L., Shuttleworth, W. J., & Valdés, J. B. (2011). Estimating evapotranspiration under warmer climates: Insights from a semi-arid riparian system. *Journal of Hydrology*, *399*(1), 1–11. https://doi.org/10.1016/j.jhydrol.2010.12.021

Shi, Z., Thomey, M. L., Mowll, W., Litvak, M., Brunsell, N. A., Collins, S. L., et al. (2014). Differential effects of extreme drought on production and respiration: Synthesis and modeling analysis. *Biogeosciences*, *11*, 621–633. https://doi.org/10.5194/bg-11-621-2014

Sivandran, G., & Bras, R. L. (2012). Identifying the optimal spatially and temporally invariant root distributions for a semiarid environment. *Water Resources Research*, *48*, W12525. https://doi.org/10.1029/2012WR012055

Slot, M., & Kitajima, K. (2015). General patterns of acclimation of leaf respiration to elevated temperatures across biomes and plant types. *Oecologia*, *177*(3), 885–900. https://doi.org/10.1007/s00442-014-3159-4

Smith, S. D., Huxman, T. E., Zitzer, S. F., Charlet, T. N., Housman, D. C., Coleman, J. S., et al. (2000). Elevated CO_2 increases productivity and invasive species success in an arid ecosystem. *Nature*, *408*(6808), 79–82. https://doi.org/10.1038/35040544

Spitters, C. J. T., Toussaint, H. A. J. M., & Goudriaan, J. (1986). Separating the diffuse and direct component of global radiation and its implications for modeling canopy photosynthesis Part I. Components of incoming radiation. *Agricultural and Forest Meteorology*, *38*(1–3), 217–229. https://doi.org/10.1016/0168-1923(86)90060-2

Sponseller, R. A. (2007). Precipitation pulses and soil CO_2 flux in a Sonoran Desert ecosystem. *Global Change Biology*, *13*(2), 426–436. https://doi.org/10.1111/j.1365-2486.2006.01307.x

Steinweg, J. M., Plante, A. F., Conant, R. T., Paul, E. A., & Tanaka, D. L. (2008). Patterns of substrate utilization during long-term incubations at different temperatures. *Soil Biology and Biochemistry*, *40*(11), 2722–2728. https://doi.org/10.1016/j.soilbio.2008.07.002

Stoy, P. C., Katul, G. G., Siqueira, M. B., Juang, J. Y., Novick, K. A., Uebelherr, J. M., & Oren, R. (2006). An evaluation of models for partitioning eddy covariance-measured net ecosystem exchange into photosynthesis and respiration. *Agricultural and Forest Meteorology*, *141*(1), 2–18. https://doi.org/10.1016/j.agrformet.2006.09.001

Stoy, P. C., Richardson, A. D., Baldocchi, D. D., Katul, G. G., Stanovick, J., Mahecha, M. D., et al. (2009). Biosphere-atmosphere exchange of CO_2 in relation to climate. *Biogeosciences*, *6*, 2297–2312. https://doi.org/10.5194/bg-6-2297-2009

Tang, Q., Vivoni, E. R., Muñoz-Arriola, F., & Lettenmaier, D. P. (2012). Predictability of evapotranspiration patterns using remotely sensed vegetation dynamics during the North American monsoon. *Journal of Hydrometeorology*, *13*(1), 103–121. https://doi.org/10.1175/JHM-D-11-032.1

Taylor, K. E., Stouffer, R. J., & Meehl, G. A. (2012). An overview of CMIP5 and the experiment design. *Bulletin of the American Meteorological Society*, *93*(4), 485–498. https://doi.org/10.1175/BAMS-D-11-00094.1

Thiessen, S., Gleixner, G., Wutzler, T., & Reichstein, M. (2013). Both priming and temperature sensitivity of soil organic matter decomposition depend on microbial biomass—An incubation study. *Soil Biology and Biochemistry*, *57*, 739–748. https://doi.org/10.1016/j.soilbio.2012.10.029

Thomey, M. L., Collins, S. L., Vargas, R., Johnson, J. E., Brown, R. F., Natvig, D. O., & Friggens, M. T. (2011). Effect of precipitation variability on net primary production and soil respiration in a Chihuahuan Desert grassland. *Global Change Biology*, *17*(4), 1505–1515. https://doi.org/10.1111/j.1365-2486.%202010.02363.x

Unger, S., Máguas, C., Pereira, J. S., David, T. S., & Werner, C. (2010). The influence of precipitation pulses on soil respiration—Assessing the "Birch effect" by stable carbon isotopes. *Soil Biology and Biochemistry*, *42*(10), 1800–1810. https://doi.org/10.1016/j.soilbio.2010.06.019

Vargas, R., Sonnentag, O., Abramowitz, G., Carrara, A., Chen, J. M., Ciais, P., et al. (2013). Drought influences the accuracy of simulated ecosystem fluxes: A model-data meta-analysis for Mediterranean oak woodlands. *Ecosystems*, *16*, 749–764. https://doi.org/10.1007/s10021-013-9648-1

Verduzco, V. S. (2016). Climate variability impacts on net ecosystem production in northwest Mexico. PhD dissertation in biotechnology, Instituto Technológico de Sonora, Ciudad Obregón, Sonora, México, 169 pp.

Verduzco, V. S., Garatuza-Payán, J., Yépez, E. A., Watts, C. J., Rodríguez, J. C., Robles-Morua, A., & Vivoni, E. R. (2015). Variations of net ecosystem production due to seasonal precipitation differences in a tropical dry forest of northwest Mexico. *Journal of Geophysical Research: Biogeosciences*, *120*, 2081–2094. https://doi.org/10.1002/2015JG003119

Villarreal, S., Vargas, R., Yepez, E. A., Acosta, J. S., Castro, A., Escoto-Rodriguez, M., et al. (2016). Contrasting precipitation seasonality influences evapotranspiration dynamics in water-limited shrublands. *Journal of Geophysical Research: Biogeosciences*, *121*, 494–508. https://doi.org/10.1002/2015JG003169

Vivoni, E. R., Entekhabi, D., Bras, R. L., Ivanov, V. Y., Van Horne, M. P., Grassotti, C., & Hoffman, R. N. (2006). Extending the predictability of hydrometeorological flood events using radar rainfall nowcasting. *Journal of Hydrometeorology*, *7*(4), 660–677. https://doi.org/10.1175/JHM514.1

Vivoni, E. R., Ivanov, V. Y., Bras, R. L., & Entekhabi, D. (2005). On the effects of triangulated terrain resolution on distributed hydrologic model response. *Hydrological Processes*, *19*(11), 2101–2122. https://doi.org/10.1002/hyp.5671

Vivoni, E. R., Moreno, H. A., Mascaro, G., Rodriguez, J. C., Watts, C. J., Garatuza-Payan, J., & Scott, R. L. (2008). Observed relation between evapotranspiration and soil moisture in the North American monsoon region. *Geophysical Research Letters*, *35*, L22403. https://doi.org/10.1029/2008GL036001

Vivoni, E. R., Rodríguez, J. C., & Watts, C. J. (2010). On the spatiotemporal variability of soil moisture and evapotranspiration in a mountainous basin within the North American monsoon region. *Water Resources Research*, *46*, W02509. https://doi.org/10.1029/2009WR008240

Vivoni, E. R., Watts, C. J., Rodríguez, J. C., Garatuza-Payan, J., Méndez-Barroso, L. A., & Saiz-Hernández, J. A. (2010). Improved land–atmosphere relations through distributed footprint sampling in a subtropical scrubland during the North American monsoon. *Journal of Arid Environments*, *74*(5), 579–584. https://doi.org/10.1016/j.jaridenv.2009.09.031

Wang, D., Heckathorn, S. A., Wang, X., & Philpott, S. M. (2012). A meta-analysis of plant physiological and growth responses to temperature and elevated CO_2. *Oecologia*, *169*(1), 1–13. https://doi.org/10.1007/s00442-011-2172-0

Watts, C. J., Scott, R. L., Garatuza-Payan, J., Rodriguez, J. C., Prueger, J. H., Kustas, W. P., & Douglas, M. (2007). Changes in vegetation condition and surface fluxes during NAME 2004. *Journal of Climate*, *20*(9), 1810–1820. https://doi.org/10.1175/JCLI4088.1

Webb, E. K., Pearman, G. I., & Leuning, R. (1980). Correction of flux measurements for density effects due to heat and water vapor transfer. *Quarterly Journal of the Royal Meteorological Society*, *106*(447), 85–100. https://doi.org/10.1002/qj.49710644707

Werk, K. S., Ehleringer, J., Forseth, I. N., & Cook, C. S. (1983). Photosynthetic characteristics of Sonoran Desert winter annuals. *Oecologia*, *59*(1), 101–105. https://doi.org/10.1007/BF00388081

Wilczak, J. M., Oncley, S. P., & Stage, S. A. (2001). Sonic anemometer tilt correction algorithms. *Boundary-Layer Meteorology*, *99*(1), 127–150. https://doi.org/10.1023/A:1018966204465

Williams, A. P., Allen, C. D., Macalady, A. K., Griffin, D., Woodhouse, C. A., Meko, D. M., et al. (2013). Temperature as a potent driver of regional forest drought stress and tree mortality. *Nature Climate Change*, *3*(3), 292–297. https://doi.org/10.1038/nclimate1693

Wu, Z., Dijkstra, P., Koch, G. W., Penuelas, J., & Hungate, B. A. (2011). Responses of terrestrial ecosystems to temperature and precipitation change: A meta-analysis of experimental manipulation. *Global Change Biology*, *17*(2), 927–942. https://doi.org/10.1111/j.1365-2486.2010.02302.x

Xiao, J., Zhuang, Q., Law, B. E., Baldocchi, D. D., Chen, J., Richardson, A. D., et al. (2011). Assessing net ecosystem carbon exchange of US terrestrial ecosystems by integrating eddy covariance flux measurements and satellite observations. *Agricultural and Forest Meteorology*, *151*(1), 60–69. https://doi.org/10.1016/j.agrformet.2010.09.002

Xie, J., Zha, T., Jia, X., Qian, D., Wu, B., Zhang, Y., et al. (2015). Irregular precipitation events in control of seasonal variations in CO_2 exchange in a cold desert-shrub ecosystem in northwest China. *Journal of Arid Environments*, *120*, 33–41. https://doi.org/10.1016/j.jaridenv.2015.04.009

Xu, C., McDowell, N. G., Sevanto, S., & Fisher, R. A. (2013). Our limited ability to predict vegetation dynamics under water stress. *New Phytologist*, *200*(2), 298–300. https://doi.org/10.1111/nph.12450

Xu, L., & Baldocchi, D. D. (2004). Seasonal variation in carbon dioxide exchange over a Mediterranean annual grassland in California. *Agricultural and Forest Meteorology*, *123*(1), 79–96. https://doi.org/10.1016/j.agrformet.2003.10.004

Xu, Z., Shimizu, H., Ito, S., Yagasaki, Y., Zou, C., Zhou, G., & Zheng, Y. (2014). Effects of elevated CO_2, warming and precipitation change on plant growth, photosynthesis and peroxidation in dominant species from North China grassland. *Planta*, *239*(2), 421–435. https://doi.org/10.1007/s00425-013-1987-9

Yamori, W., Hikosaka, K., & Way, D. A. (2014). Temperature response of photosynthesis in C_3, C_4, and CAM plants: Temperature acclimation and temperature adaptation. *Photosynthesis Research*, *119*(1–2), 101–117. https://doi.org/10.1007/s11120-013-9874-6

Yang, Y., Guan, H., Batelaan, O., McVicar, T. R., Long, D., Piao, S., et al. (2016). Contrasting responses of water use efficiency to drought across global terrestrial ecosystems. *Scientific Reports*, *6*, 23,284. https://doi.org/10.1038/srep23284

Yépez, E. A., Scott, R. L., Cable, W. L., & Williams, D. G. (2007). Intraseasonal variation in water and carbon dioxide flux components in a semiarid riparian woodland. *Ecosystems*, *10*(7), 1100–1115. https://doi.org/10.1007/s10021-007-9079-y

Zhang, X., Niu, G. Y., Elshall, A. S., Ye, M., Barron-Gafford, G. A., & Pavao-Zuckerman, M. (2014). Assessing five evolving microbial enzyme models against field measurements from a semiarid savannah—What are the mechanisms of soil respiration pulses? *Geophysical Research Letters*, *41*, 6428–6434. https://doi.org/10.1002/2014GL061399

Zhou, X., Wan, S., & Luo, Y. (2007). Source components and interannual variability of soil CO_2 efflux under experimental warming and clipping in a grassland ecosystem. *Global Change Biology*, *13*(4), 761–775. https://doi.org/10.1111/j.1365-2486.2007.01333.x

Zhou, Z., Jiang, L., Du, E., Hu, H., Li, Y., Chen, D., & Fang, J. (2013). Temperature and substrate availability regulate soil respiration in the tropical mountain rainforests, Hainan Island, China. *Journal of Plant Ecology*, *6*(5), 325–334. https://doi.org/10.1093/jpe/rtt034